Aus dem Department/Klinik für Kleintiere und Pferde

der Veterinärmedizinischen Universität Wien

Institut/Klinik für Kleintierchirurgie, Augen- und Zahnheilkunde

Leiter: O.Univ.Prof. Dr. Gilles Dupre, Dipl.ECVS

Evaluation of the femoral and tibial alignments in dogs: A systematic review

Diplomarbeit

Veterinärmedizinischen Universität Wien

vorgelegt von

Masoud Aghapour, DVM

Wien, im Dezember 2019

Betreuerin

Ass.-Prof. Dr.med.vet Britta Vidoni

Fachtierärztin für Chirurgie, Klein- und Heimtiere

Gutachter

Ao.Univ.-Prof. Dr.med.vet. Sibylle Kneissl

Vizerektorin für Lehre

Oberärztin, Administrative Leitung der Abteilung für Bildgebende Diagnostik

Danksagung

An dieser Stelle möchte ich mich von ganzem Herzen bei meinen großartigen Betreuerinnen Frau Ass.-Prof. Dr. Britta Vidoni und Frau Priv.-Doz. Dr. Barbara Bockstahler bedanken. Sie haben mich mit viel Geduld durch diese Arbeit geführt und waren zu jeder Zeit bei der Lösung vieler kleiner und auch größerer Probleme stets behilflich. Ein ganz besonderer Dank gilt Herrn Prof. Dr. Gilles Dupré für die Unterstützung dieses Projekts.

Wien, im Dezember 2019 Masoud Aghapour

Table of Content

List of Tables

List of Figures

Abbreviations

3D	three-dimensional
AA	angle of anteversion or femoral torsion angle
aCdDFA	anatomic caudal distal femoral angle
aCdPFA	anatomic caudal proximal femoral angle
aLDFA	anatomic lateral distal femoral angle
aLPFA	anatomic lateral proximal femoral angle
AMA-angle	anatomical-mechanical axis angle
CdC–CdT	caudal condylar and distal caudal tibial axis pair
CdC–CnT	caudal condylar and distal cranial tibial axis pair
CrCL	cranial cruciate ligament
CT	computed tomography
CTA	crural torsion angle
DAA	distal angle of anteversion
DMTCA	distal medial tibial cortex angle
DPA	distal tibial axis/proximal tibial axis angle or diaphyseal proximal tibial angle
DTW	diaphyseal tibial width
FAA	femoral anteversion angle
FCT	femoral trochanteric angle
FFA	frontal angle of the femoral neck
FNA	femoral neck angle
FNA	angle femoral neck anteversion angle
FPA	frontal plane alignment
FVA	femoral varus angle
ICA	angle of inclination
LPL	lateral patellar luxation
MAFA	mechanical axis—femur angle
MAMTA	mechanical axis—metatarsal angle
mCdDFA	mechanical caudal distal femoral angle
mCdDTA	mechanical caudal distal tibial angle
mCdPFA	mechanical caudal proximal femoral angle

mCdPTA	mechanical caudal proximal tibial angle
mCrDTA	mechanical cranial distal tibial angle
mCrPTA	mechanical cranial proximal tibial angle
mLDFA	mechanical lateral distal femoral angle
mLDTA	mechanical lateral distal tibial angle
mLPFA	mechanical lateral proximal femoral angle
mLPTA	mechanical lateral proximal tibial angle
mMDTA	mechanical medial distal tibial angle
mMPTA	mechanical medial proximal tibial angle
mMTTA	mechanical metatarsotibial angle
MPL	medial patellar luxation
MTCT	medial tibial cortex torsion
mTFA	mechanical tibiofemoral angle
PA	procurvation angle or Procurvatum angle
PAA	proximal angle of anteversion
PMTCA	proximal medial tibial cortex angle
PTA	patellar tendon angle
PTL	proximal tibial length
PTTA	proximal tibial tuberosity angle
PTW	proximal tibial width
Q angle	quadriceps angle
rTTW	relative tibial tuberosity width
SMAD	stifle mechanical axis deviation
SPA	sagittal plane alignment
TC–CdT	transcondylar and distal caudal tibial axis pair
TC-CnT	transcondylar and distal cranial tibial axis pair
TMAD	tarsal mechanical axis deviation
TPA	tibial plateau angle
TPL	tibial plateau length
TPO	tibial plateau orientation
TPS	tibial plateau slope

TTA	tibial torsion angle
TTD	tibial tuberosity displacement
TV	tibial valgus

1 Introduction

Evaluation of the fore and hind limb conformations and clinical goniometry were always important topics in veterinary orthopedics as it is in human medicine. Cognition of reference values of pelvic limb alignments, including anatomic and mechanical angles of the femur and tibia would help the veterinarian to specify the quantitative degree of malalignments. In human medicine, different methods were developed during the years (1976 to 2018) to quantify the grade of the limb deformities (Paley 2003). Using standard methods in the measurement of the alignments provides reliable and homogenous values for the surgeons and allows them to use the reported scales in the literature, especially in the case of bilateral deformities, where the sound extremity does not exist as a reference proportion. Normal limb alignments may be varying in different dog breeds or between large and small breed dogs, therefore determination of reference ranges for different dog breeds is important.

Angular deformities of the canine hind limb were mostly reported to occur in the femur, tibia, and metatarsus. These deformities usually develop after premature total or partial closure of a physis (Vaughan 1976, Marretta and Schrader 1983, Ramadan and Vaughan 1979, Johnson et al. 1989, Jaeger et al. 2007, Altunatmaz et al. 2007, Burton and Owen 2007, McCarthy 1998, Nelligan et al. 2010). Physeal damage can occur because of various causes, including trauma, nutritional imbalances, hypertrophic osteodystrophy (metaphyseal osteopathy), retained cartilage cores, radiation and iatrogenic reasons like an improper application of a fixation apparatus (Morgan and Miller 1994, Conzemius et al. 1994, Kettelkamp et al. 1988). Abnormal pressure on the distal femoral physis can cause angular deformity of the femur (Hulse 1993). Most of the canine femurs may have some degrees of varus. Distal femoral varus is defined as the angulation of the distal femur inward the body. Abnormal distal femoral varus associates with medial patellar luxation (Hulse 1993). Angular deformity of the femur in the frontal plane (varus/valgus) can be diagnosed by joint reference angles, including the anatomic and mechanical proximal or distal femoral angles. The joint reference angle is an angle between the bone axis and its respective joint orientation line (Paley 2003). The bone axis may be the mechanical or anatomic axis. The mechanical axis is a straight line, connecting the centers of the proximal and distal joints of the bone. Anatomic axis is a straight or curved line that passes through the center of the bone (Paley 2003).

Bone deformities in the canine pelvic limb are not limited to the femur. Pes varus and valgus describe skeletal deformities, characterized by a medial and lateral deviation of the distal tibia in the frontal plane, respectively (Altunatmaz et al. 2007, Burton and Owen 2007, McCarthy 1998). The etiology of this skeletal deformity is an asymmetric growth of the distal tibial physis because of traumatic, nutritional or developmental premature closure of the physis (Ramadan and Vaughan 1979, Johnson et al. 1989, Burton and Owen 2007).

Different studies carried out during the last years to evaluate the hind limb alignments of the dogs. Some of these studies have been focused on developing standard methods for the measurements of the hind limb conformations (Aper et al. 2005, Dudley et al. 2006, Osmond et al. 2006, Tomlinson et al. 2007, Dismukes et al. 2007, Dismukes et al. 2008a, Dismukes et al. 2008b, Mostafa et al. 2008, Lambert and Wendelburg 2010, Lojszczyk-Szczepaniak et al. 2014, Sabanci and Ocal 2014, Witte 2015, Hette et al. 2016, Savio et al. 2016, Pinna and Romagnoli 2017, Kara et al. 2018). Some studies have been compared the alignments in dogs with and without the different orthopedic diseases (Hette et al. 2016, Sarierler 2004, Mortari et al. 2009, Ragetly et al. 2011, Fitzpatrick et al. 2012, Soparat et al. 2012, Vedrine et al. 2013, Pinna et al. 2013, Fuller et al. 2014, Aertsens et al. 2015, Su et al. 2015, Olimpo et al. 2016, Yasukawa et al. 2016, Guénégo et al. 2017, Janovec et al. 2017, Lusetti et al. 2017, Newman and Voss 2017, Perry et al. 2017, Garnoeva et al. 2018, Phetkaew et al. 2018, Žilinčík et al. 2018). The next group was the studies with a focus on the accuracy of the reported methods. These studies evaluated different methods for the same parameters to assess the effect of the examiner and tools on the results (Aper et al. 2005, Dudley et al. 2006, Osmond et al. 2006, Ginja et al. 2007, Swiderski et al. 2008, Glassman et al. 2011, Palmer et al. 2011, Jackson and Wendelburg 2011, Oxley et al. 2013, Mostafa et al. 2014, Barnes et al. 2015, Miles et al. 2015, Longo et al. 2018, Mostafa et al. 2018).

The current review focuses on the previously performed studies involving standardized methods of measurement and terminology of pelvic limb alignments in dogs. The aims of this review were to evaluate each alignment that has been reported in the articles separately to 1) report standard values; 2) compare the measured values in dogs with and without different orthopedic diseases; 3) evaluate the repeatability and reproducibility of the reported protocols.

2 Material and methods

The standard guideline for reporting systematic reviews was used in this study (Moher et al. 2009). All articles were collected by screening the databases Scopus, PubMed and Web of the Science on 24 September 2018. The Scopus search for the Term ‘alignment or malalignment or angle or angular value’ yielded 2,625,647 articles. The search for the terms ‘dog or canine’ yielded 1,300,714 articles. The search for the terms ‘hind limb or pelvic limb or extremity’ yielded 438,229 articles. The search for the terms ‘femur or femoral’ and ‘tibia or tibial’ yielded 431,116 and 209,343 articles respectively. The combination of these search results narrowed the number of articles down to 663. The numbers of these articles were narrowed down to 403 by using the filters ‘veterinary medicine, medicine, and agricultural and biological science’. After excluding the unrelated articles to the study (unrelated diagnostic imaging articles: 19, anatomy, histology and embryology: 11, kinematic and rehabilitation: 27, other species: 39, human medicine: 130, genetics: 3, anesthesiology: 5, surgical methods: 58, regenerative medicine: 10, forelimb alignments: 6 and other disease: 56) the final number was narrowed down to the 38 articles. The same procedures were performed for PubMed and Web of the Science databases. The final number of the articles from PubMed yielded 15 articles and from Web of the Science yielded 23 articles; furthermore, 47 articles from references and other sources were added to the list. After excluding the duplicate articles, the titles and abstracts of the selected articles were evaluated, and unrelated articles were excluded. The final evaluation was carried out with reading full-text of remained 68 articles and 47 articles were included in the systematic review. The number of the included articles and the exclusion process are explained in figure 1.

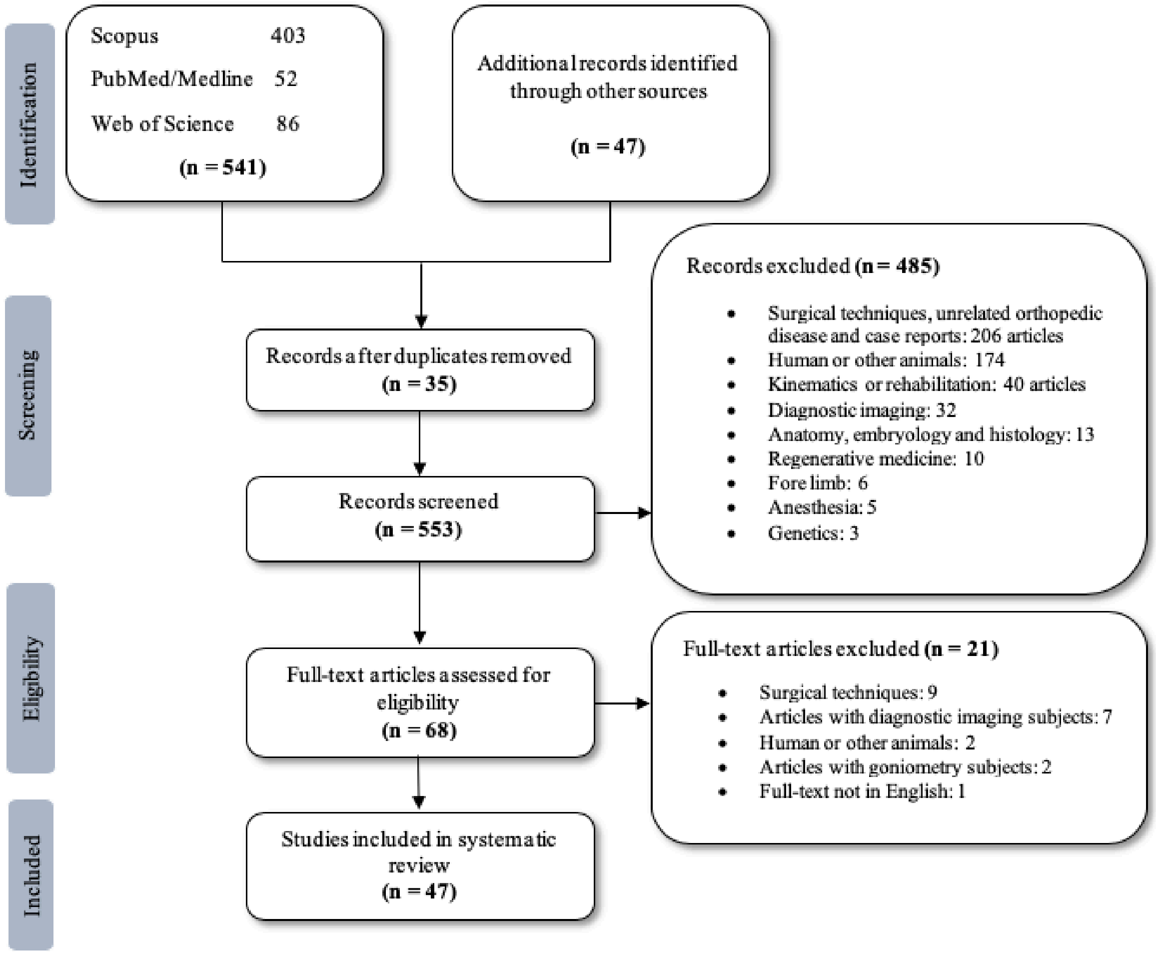

Figure 1. The numbers of identified articles and the exclusion process.

3 Results

3.1 Study overviews

According to the purpose of the studies, articles were classified into three main categories. The first category was the articles that focused on reporting standard methods for measurements of femoral and tibial alignments or reporting reference values (Aper et al. 2005, Dudley et al. 2006, Osmond et al. 2006, Tomlinson et al. 2007, Dismukes et al. 2007, Dismukes et al. 2008a, Dismukes et al. 2008b, Mostafa et al.2008, Lambert and Wendelburg 2010, Lojszczyk-Szczepaniak et al. 2014, Sabanci and Ocal 2014, Witte 2015, Hette et al. 2016, Savio et al. 2016, Pinna and Romagnoli 2017, Kara et al. 2018). Sixteen articles from a total of 46 articles were included in this category. The second category was the studies that compared the femoral and tibial alignments in different dog breeds or in dogs with and without different orthopedic diseases such as dogs with cranial cruciate ligament (CrCL) rupture, different grades of medial or lateral patellar luxation (MPL or LPL) and dogs with osteoarthritis (Hette et al. 2016, Sarierler 2004, Mortari et al. 2009, Ragetly et al. 2011, Fitzpatrick et al. 2012, Soparat et al. 2012, Vedrine et al. 2013, Pinna et al. 2013, Fuller et al. 2014, Aertsens et al. 2015, Su et al. 2015, Olimpo et al. 2016, Yasukawa et al. 2016, Guénégo et al. 2017, Janovec et al. 2017, Lusetti et al. 2017, Newman and Voss 2017, Perry et al. 2017, Garnoeva et al. 2018, Phetkaew et al. 2018, Žilinčík et al. 2018). Twenty-one articles were contained in the second category. The third category was the studies that evaluated the intra- and inter-observer agreements for reported methods or compared different diagnostic imaging tools and measurement methods. The main goal of these studies was to evaluate the effect of different methods, tools or observers on measured values (Aper et al. 2005, Dudley et al. 2006, Osmond et al. 2006, Ginja et al. 2007, Swiderski et al. 2008, Glassman et al. 2011, Palmer et al. 2011, Jackson and Wendelburg 2011, Oxley et al. 2013, Mostafa et al. 2014, Barnes et al. 2015, Miles et al. 2015, Longo et al. 2018, Mostafa et al. 2018). Fourteen studies were included in the third category. Most of the included studies had several purposes, therefore, some articles were categorized at the same time in different groups (Aper et al. 2005, Dudley et al. 2006, Osmond et al. 2006, Hette et al. 2016)

3.2 Imaging methods

Different imaging methods were carried out to measure the hind limb alignments such as radiography, computed tomography (CT), digital photography and three-dimensional (3D) scanning. In some studies, measurements were done with only one imaging method, though in some studies different imaging techniques were compared. The number of studies with different imaging methods is shown in table1.

Table 1. Classification of the included articles, according to the imaging method.

Imaging method	Number of articles
Radiography	26
Computed tomography	8
Radiography vs. Computed tomography	7
Radiography vs. Photography	3
Computed tomography vs. Photography	1
Digital Photography	1
Three-dimensional scanning	1

3.3 Animals

Different dog breeds were evaluated in the included studies. The main aim of these studies was to figure out whether the different dog breeds had significantly different hind limb alignments. In general, the articles could be divided into studies on small and large breed dogs; however, some studies were evaluated a combination of small, medium and large breed dogs. Ten Studies were performed on large breed dogs (Aper et al. 2005, Tomlinson et al. 2007, Lojszczyk-Szczepaniak et al. 2014, Ragetly et al. 2011, Pinna et al. 2013, Guénégo et al. 2017, Ginja et al. 2007, Palmer et al. 2011, Mostafa et al. 2014, Mostafa et al. 2018). Two studies were performed on medium breeds (Lusetti et al. 2017, Newman and Voss 2017). Nine studies were evaluated small breed dogs (Witte 2015, Fitzpatrick et al. 2012, Soparat et al. 2012, Olimpo et al. 2016, Yasukawa et al. 2016, Janovec et al. 2017, Garnoeva et al. 2018, Phetkaew et al. 2018, Žilinčík et al. 2018) and 26 studies were evaluated combination of small and large breeds (Dudley et al. 2006, Osmond et al. 2006, Dismukes et al. 2007, Dismukes et al. 2008a, Dismukes et al. 2008b, Mostafa et al. 2008, Lambert and Wendelburg 2010, Sabanci and Ocal 2014, Hette et al. 2016, Savio et al. 2016, Pinna and Romagnoli 2017, Kara et al. 2018, Sarierler 2004, Mortari et al. 2009, Vedrine et al. 2013, Fuller et al. 2014, Aertsens et al. 2015, Su et al. 2015, Perry et al. 2017, Swiderski et al. 2008, Glassman et al. 2011, Jackson and Wendelburg 2012, Oxley et al. 2013, Barnes et al. 2015, Miles et al. 2015, Longo et al. 2018). The population and breeds of the dogs included in the literature are shown in figure 2.

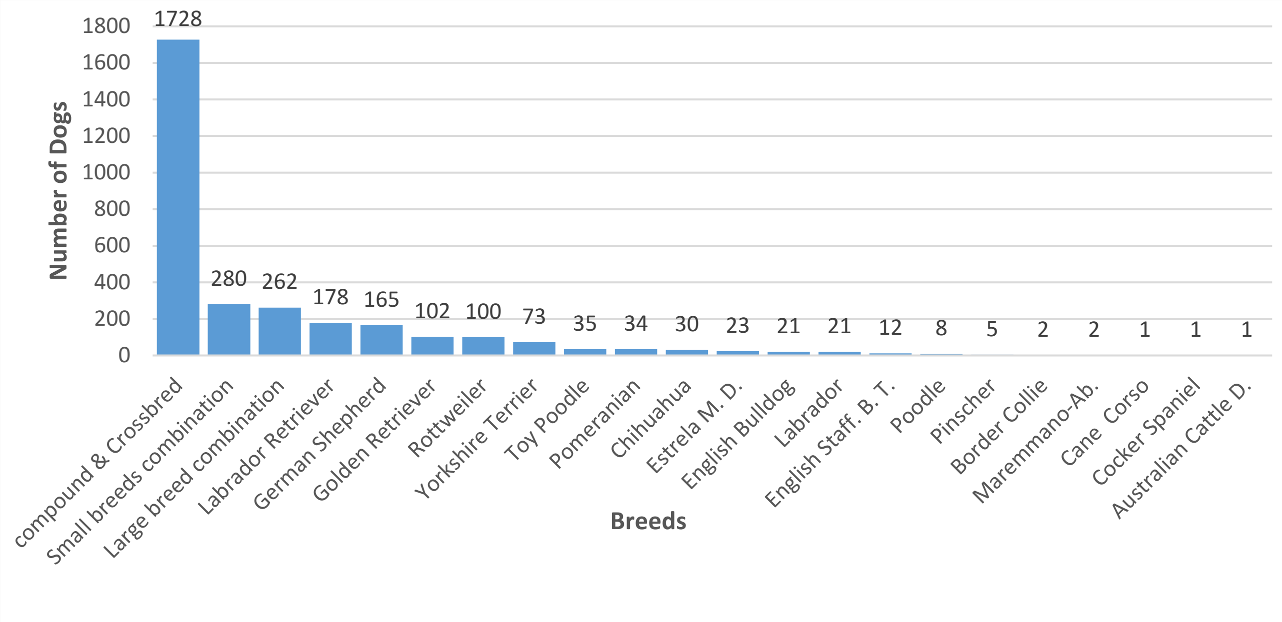

Figure 2. Classification of the included articles, according to the dog breeds**.**

In 11 studies measurements were carried out on cadaveric specimen (Aper et al. 2005, Dudley et al. 2006, Osmond et al. 2006, Dismukes et al. 2008a, Lambert and Wendelburg 2008, Savio et al. 2016, Kara et al. 2018, Swiderski et al. 2008, Palmer et al. 2011, Jackson and Wendelburg 2012, Miles et al. 2015). In the included studies, the dogs had different health conditions, 17 studies were reported the measured values in healthy dogs (Aper et al. 2005, Dudley et al. 2006, Tomlinson et al. 2007, Lambert and Wendelburg 2010, Lojszczyk-Szczepaniak et al. 2014, Sabanci and Ocal 2014, Witte 2015, Savio et al. 2016, Pinna and Romagnoli 2017, Kara et al. 2018, Vedrine et al. 2013, Ginja et al. 2007, Swiderski et al. 2008, Palmer et al. 2011, Jackson and Wendelburg 2012, Miles et al. 2015, Longo et al. 2018) , however 30 studies investigated the dogs with and without different orthopedic disease such as cranial cruciate ligament rupture (Osmond et al. 2006, Dismukes et al. 2007, Dismukes et al. 2008a, Dismukes et al. 2008b, Ragetly et al. 2011, Fuller et al. 2014, Aertsens et al. 2015, Su et al. 2015, Guénégo et al. 2017, Janovec et al. 2017, Glassman et al. 2011, Mostafa et al. 2014, Mostafa et al. 2018), different grades of medial or lateral patellar luxation (Mostafa et al. 2008, Mortari et al. 2009, Fitzpatrick et al. 2012, Soparat et al. 2012, Olimpo et al. 2016, Yasukawa et al. 2016, Lusetti et al. 2017, Newman and Voss 2017, Perry et al. 2017, Garnoeva et al. 2018, Phetkaew et al. 2018, Žilinčík et al. 2018, Barnes et al. 2015) and other orthopedic disease related to the femur, tibia or stifle joint (Hette et al. 2016, Sarierler 2004, Pinna et al. 2013, Oxley et al. 2013). The main goal of these studies was to assess the influence of mentioned orthopedic disease on hind limb alignments.

3.4 Alignments

Femoral and tibial alignments were divided into the alignments in the frontal, lateral and transverse planes. In general, 17 femoral alignments and 38 tibial alignments were measured in the literature. The investigated alignments for the femur and tibia in the frontal, sagittal and axial plane are shown in table 2, furthermore, the list of measured alignments is summarized in table 3 according to the article and author.

Table 2. Femoral and tibial alignments in the frontal, sagittal and axial plane.

Bone	Plane	Alignments
Femur	Frontal	ICA or FNA, aLPFA, mLPFA, aLDFA, mLDFA, FVA, Q angle, *FNA angle or FAA, MAFA, SMAD
	Sagittal	aCdPFA, mCdPFA, aCdDFA, mCdDFA, PA, *FNA angle
	Axial	AA, FAA
Tibia	Frontal	mMPTA, mMDTA, mLPTA, mLDTA, mTFA, MAMTA, mMTTA, TMAD, FPA, TV
	Sagittal	TPA, DPA, Z angle, rTTW, mCrPTA, mCdPTA, mCrDTA, mCdDTA, TPS, TPO, SPA, PTA, AMA-angle, PTTA, TPL, PTW, DTW, PTL
	Axial	TTD, CTA, TTA, PMTCA, DMTCA, MTCT, TC-CnT, TC–CdT, CdC–CnT, CdC–CdT

* FNA angle is measured in both frontal and sagittal planes

AA (angle of anteversion or femoral torsion angle), aCdDFA (anatomic caudal distal femoral angle), aCdPFA (anatomic caudal proximal femoral angle), aLDFA (anatomic lateral distal femoral angle), aLPFA (anatomic lateral proximal femoral angle), AMA-angle (anatomical-mechanical axis angle), CdC–CdT (caudal condylar and distal caudal tibial axis pair), CdC–CnT (caudal condylar and distal cranial tibial axis pair), CTA (crural torsion angle), DAA (distal angle of anteversion), DMTCA (distal medial tibial cortex angle), DPA (distal tibial axis/proximal tibial axis angle or diaphyseal proximal tibial angle), DTW (diaphyseal tibial width), FAA (femoral anteversion angle), FCT (femoral trochanteric angle), FFA (Frontal angle of the femoral neck), FNA (femoral neck angle), FNA angle (femoral neck anteversion angle), FPA (frontal plane alignment), FVA (femoral varus angle), ICA (angle of inclination), MAFA (mechanical axis—femur angle), MAMTA (mechanical axis—metatarsal angle), mCdDFA (mechanical caudal distal femoral angle), mCdDTA (mechanical caudal distal tibial angle), mCdPFA (mechanical caudal proximal femoral angle), mCdPTA (mechanical caudal proximal tibial angle), mCrDTA (mechanical cranial distal tibial angle), mCrPTA (mechanical cranial proximal tibial angle), mLDFA (mechanical lateral distal femoral angle), mLDTA (mechanical lateral distal tibial angle), mLPFA (mechanical lateral proximal femoral angle), mLPTA (mechanical lateral proximal tibial angle), mMDTA (mechanical medial distal tibial angle), mMPTA (mechanical medial proximal tibial angle), mMTTA (mechanical metatarsotibial angle), MTCT (medial tibial cortex torsion), mTFA (mechanical tibiofemoral angle), PA (procurvation angle), PAA (proximal angle of anteversion), PMTCA (proximal medial tibial cortex angle), PTA (patellar tendon angle), PTL (Proximal tibial length), PTTA (proximal tibial tuberosity angle), PTW (Proximal tibial width), Q angle (quadriceps angle), rTTW (relative tibial tuberosity width), SMAD (Stifle mechanical axis deviation), SPA (sagittal plane alignment), TC-CnT (transcondylar and distal cranial tibial axis pair), TC–CdT (transcondylar and distal caudal tibial axis pair), TMAD (Tarsal mechanical axis deviation), TPA (tibial plateau angle), TPL (tibial plateau length), TPO (tibial plateau orientation), TPS (tibial plateau slope), TTA (tibial torsion angle), TTD (tibial tuberosity displacement), TV (tibial valgus), Z angle.

Table 3. Measured femoral and tibial alignments in the literature.

Author	Alignments
Aertsens et al. 2015	TPA, rTTW, Z angle
Aper et al. 2005	Tibial torsion angles (TC-CnT, TC-CdT, CdC-CnT, CdC-CdT)
Barnes et al. 2015	aLDFA, AA, mMPTA, TTD, CTA
Dismukes et al. 2007	mMPTA, mMDTA
Dismukes et al. 2008a	mLPFA, mLDFA, mMPTA, mMDTA, mTFA, mMTTA, MAFA, MAMTA, SMAD, TMAD
Dismukes et al. 2008b	mCrDTA, mCdPTA
Dudley et al., 2006	FVA, AA
Fitzpatrick et al. 2012	TTA
Fuller et al. 2014	TPA, mCaPTA, mCrDTA, SPA, FPA, mMPTA, mMDTA
Garnoeva et al. 2018	aLPFA, mLPFA, aLDFA, mLDFA, FVA, IFA, Q angle
Ginja et al. 2007	FNA angle
Glassman et al. 2011	TPA, DPA
Guénégo et al. 2017	AMA, TPA, rTTW, Z angle
Hette et al. 2016	Medial tibial cortex torsion (MTCT)
Jackson & Wendelburg 2012	aLDFA
Janovec et al. 2017	sTPA, nTPA, PTTA, TPL/DTW, PTW, DTW, PTW/TPL, nTPA/PTW, rTTW, nTPA/PTWq, rBW
Kara et al. 2018	aLDFA, CDFA, AVA, NSA
Lambert & Wendelburg 2010	mMPTA, TPA
Łojszczyk-Szczepaniak et al. 2014	Q angle
Longo et al. 2018	aLDFA, FNA, FTA
Lusetti et al. 2017	aLPFA, aLDFA, mLPFA, mLDFA, ICA, AA, mMPTA, mMDTA, mCdDTA, mCdPTA, TTA
Miles et al. 2015	aLDFA
Mostafa et al. 2018	TPA, FAA
Mostafa et al. 2008	Length & alignment of the patella, Proximal Tibia & Distal Femur
Mostafa et al. 2014	AA
Mortari et al. 2009	ICA, Norberg angle, Q angle, FVA
Newman & Voss 2017	ICA, AA, DAA, PAA, FVA, TVA, TTA, aLDFA, FCT, TV, TT
Olimpo et al. 2016	aLPFA, aLDFA, mLPFA, mLDFA, Femoral Anteversion, mCaPTA, mCrDTA, mMPTA, mMDTA, TPA
Osmond et al. 2006	TPS, TPO, DPA
Oxley et al. 2013	FVA (intra-&inter-ob.)
Palmer et al. 2011	S-aLDFA & R-aLDFA (intra-&inter-ob.)
Perry et al. 2017	FVA, aLDFA, mLDFA, ICA
Phetkaew et al. 2018	aLPFA, aLDFA, mLPFA, mLDFA, ICA, mMPTA, mMDTA, PA, mCdPTA, mCrDTA, aCdPFA, aCdDFA
Pinna et al. 2013	Norberg angle, ICA
Pinna & Romagnoli 2017	Q Angle
Ragetly et al. 2011	TPA, FAA (FNA angle)
Sabanci & Ocal 2014	TPA
Sarierler 2004	ICA
Savio et al. 2016	aLPFA, mLPFA, aLDFA, mLDFA, FNA, FTA, FVA
Soparat et al. 2012	ICA, FVA, aLDFA, mLDFA
Su et al. 2015	TPA
Swiderski et al. 2008	FVA
Tomlinson et al. 2007	aLPFA, mLPFA, aLDFA, mLDFA, ICA
Vedrine et al. 2013	TPA, PTA, Z angle, DPA, rTTW
Witte 2015	TPA, DPA, PTA, Z angle, rTTW
Yasukawa et al. 2016	aLPFA, mLPFA, aLDFA, mLDFA, FVA, IFA, PA, mCdPFA, mCdDFA, aCdPFA, aCdDFA, AA, FFA, mMPTA, mMDTA, mCrPTA, mCrDTA, TPA, Z angle, rTTW, TTA, MDTT/PTW
Žilinčík et al. 2018	aLPFA, aLDFA, AA, FIA (ICA), FVA

All abbreviations are listed in the page 8, table 2.

3.5 Measurement methods

3.5.1 Femoral angle of inclination

Measurement of the femoral neck angle or angle of inclination (ICA) described by Tomlinson et al. 2007 is shown in figure 3.

1. To identify the center of the head of the femur, draw a circle centered over the femoral head so that it matches the outline of the bone in at least 3 points. The center of the circle is point **A.**
2. Identify the midpoint of the femoral neck at its narrowest point **B.**
3. The axis of the femoral neck is represented by a straight line (**ca**) passing through points **A** and **B.**
4. Measure the length of the femur from the proximal point to the distal point in the frontal plane.
5. Identify the 1/2 of the length of the femur (Point **C**) and proximal 1/3 of the length of the femur (Point **D**).
6. Identify the midpoint of the mediolateral cortices of the femur in point **C** and **D** (remain within the cortex).
7. Draw the proximal anatomic axis (**paa**), which represented by a straight line passing through points **C** and **D**.
8. The femoral neck angle or the angle of inclination is the angle formed between the proximal anatomical axis (**paa**) and the axis of the femoral neck (**ca**).

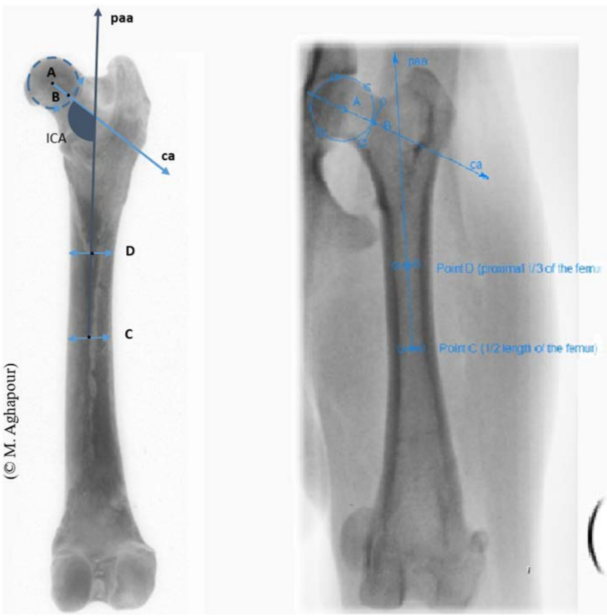

Figure 3. The femoral angle of inclination described by Tomlinson.

Measurement of the femoral neck angle or angle of inclination by SYMAX method described by Rumph and Hathcock 1990 is shown in figure 4.

1. Draw a circle centered over the femoral head so that it matches the outline of the bone in at least 3 points, the center of the circle is point **A**.
2. Draw a circle in the proximal metaphysis of the femur so that it matches the outline of the femur in at least 3 points, the center of the circle is point **B**.
3. Draw a circle in the distal meta- and epiphysis of the femur so that it matches the outline of the femur in at least 3 points, the center of the circle is point **C**.
4. Draw the anatomical axis of the femur (**aa**), which represented by a straight line passing through points **B** and **C**.
5. Draw the cervical axis of the femur (**ca**), which represented by a straight line passing through points **A** and **B**.
6. The angle of inclination is the angle formed between the anatomical axis (**aa**) and the cervical axis (**ca**) of the femur in the frontal plane.

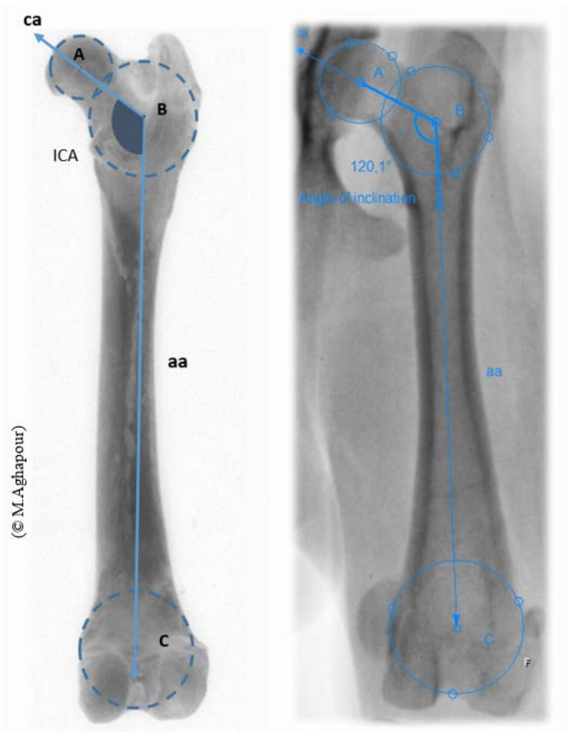

Figure 4. The femoral angle of inclination by SYMAX method.

3.5.2 Anatomic lateral proximal femoral angle and anatomic lateral distal femoral angle

Measurements of aLPFA and aLDFA (Paley 2003, Tomlinson 2007) are shown in figure 5.

1. Draw a circle centered over the femoral head so that it matches the outline of the bone in at least 3 points. The center of the circle is point **A**.
2. Draw proximal joint orientation line (**j**) by identifying the proximal tip of the greater trochanter (point **B**) and drawing a straight line passing through points **A** and **B**.
3. Draw distal joint orientation line (**k**) by identifying the most distal convexities of the femoral condyles (**P** & **P′**) and drawing a straight line connecting points P and P′.
4. Measure the length of the femur from proximal point to the distal point in the frontal plane to identify the halfway down the length of the femur (Point **C**) and proximal 1/3 of the length of the femur (Point **D**).
5. Identify the midpoint of the mediolateral cortices of the femur in point **C** and D (remain within the cortex).
6. Draw the proximal anatomical axis (**aa**), which represented by a straight line passing through points C and D and joint orientation lines.
7. The angle between the proximal joint orientation line and anatomical axis in the lateral side is the anatomical lateral proximal femoral angle (**aLPFA**) and the angle between the distal joint orientation line and anatomical axis in the lateral side is the anatomical lateral distal femoral angle (**aLDFA**).

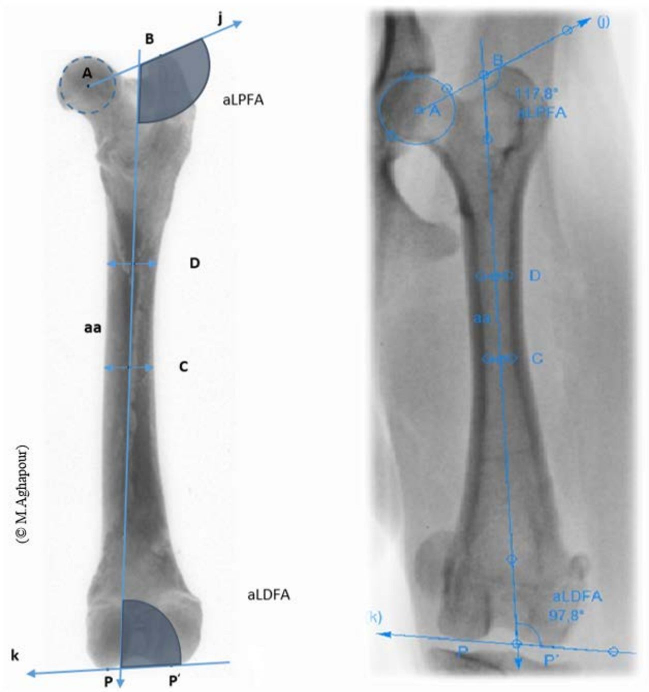

Figure 5. Anatomic lateral proximal femoral angle and anatomic lateral distal femoral.

3.5.3 Mechanical lateral proximal femoral angle and mechanical lateral distal femoral angle

Measurements of mLPFA and mLDFA (Paley 2003, Tomlinson 2007) are shown in figure 6.

1. Draw a circle centered over the femoral head so that it matches the outline of the bone in at least 3 points. The center of the circle is point **A**.
2. Draw proximal joint orientation line (**j**) by identifying the proximal tip of the greater trochanter (point **B**) and drawing a straight line passing through points A and B.
3. Draw distal joint orientation line (**k**) by identifying the most distal convexities of the femoral condyles (**P** & **P′**) and drawing a straight line connecting points P and P′.
4. Draw the mechanical axis in the frontal plane, which is a straight line (**ma**) connecting the center of the proximal joint (**A**) with the center of the distal joint.
5. The angle between the proximal joint orientation line (**j**) and mechanical axis (**ma**) in the lateral side is the mechanical lateral proximal femoral angle (**mLPFA**) and the angle between distal joint orientation line (**k**) and mechanical axis (**ma**) in the lateral side is the mechanical lateral distal femoral angle (**mLDFA**).

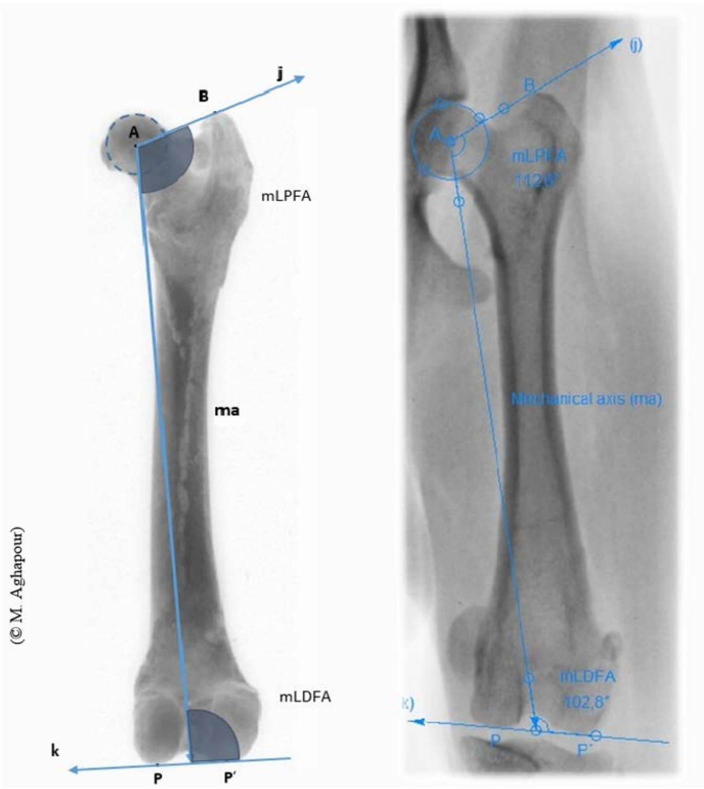

Figure 6. Mechanical lateral proximal femoral angle and mechanical lateral distal femoral.

3.5.4 Femoral varus angle

Measurement of the FVA (Paley 2003, Dudley et al. 2006) is shown in figure 7.

1. Draw distal joint orientation line (**k**) by identifying the most distal convexities of the femoral condyles (**P & P′**) and drawing a straight line connecting points P and P′.
2. Measure the length of the femur from the proximal point to the distal point in the frontal plane to identify the halfway down the length of the femur and proximal 1/3 of the length of the femur.
3. Identify the midpoint of the mediolateral cortices of the femur in proximal ⅓ (**D**) and ½ (**C**) of the length of the femur (remain within the cortex).
4. Draw the anatomical axis (**aa**), which represented by a straight line passing through points **C** and **D** and distal joint orientation line.
5. Draw a **perpendicular line** to the distal joint orientation line in the intersection point of the anatomical axis (**aa**) and the distal joint orientation line (**k**).
6. The **femoral varus angle** is the angle between the anatomic axis (**aa**) and the perpendicular line.

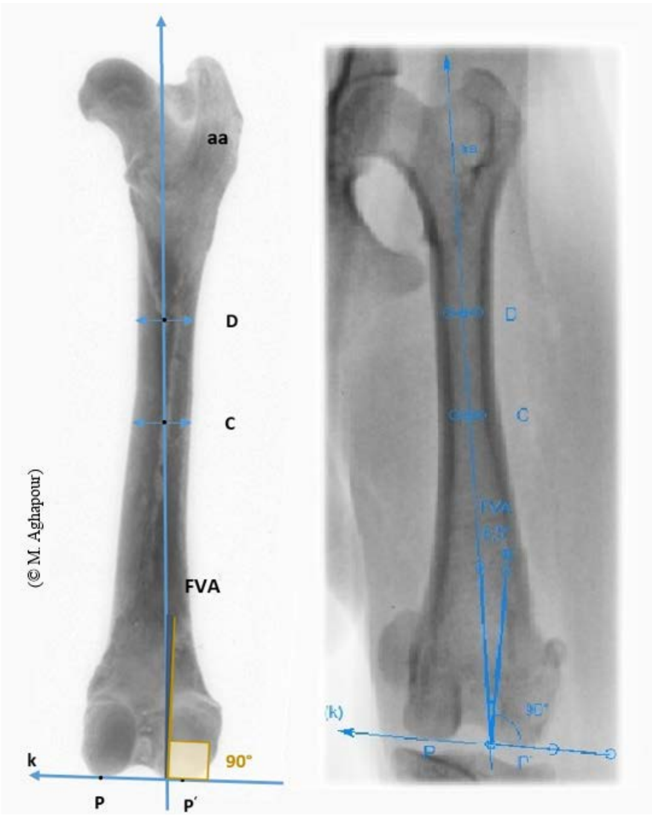

Figure 7. Femoral varus angle.

3.5.5 Femoral angle of anteversion

Measurement of the AA (Nunamaker et al. 1973) is shown in figure 8.

1. Draw a circle centered over the femoral head so that it matches the outline of the bone in at least 3 points. The center of the circle is point **A**.
2. Identify the midpoint of the femoral neck at its narrowest point between the cranial and caudal cortices of the femoral neck (**B**).
3. The cervical axis is represented by a line (**ca**) passing through the center of the point **A** and **B.**
4. Draw lines (**Z**) and (**Z´**) that is tangent to the distal articular surface of the femoral condyles.
5. The **angle of anteversion** is the angle between (**Z**) and (**ca**) line.

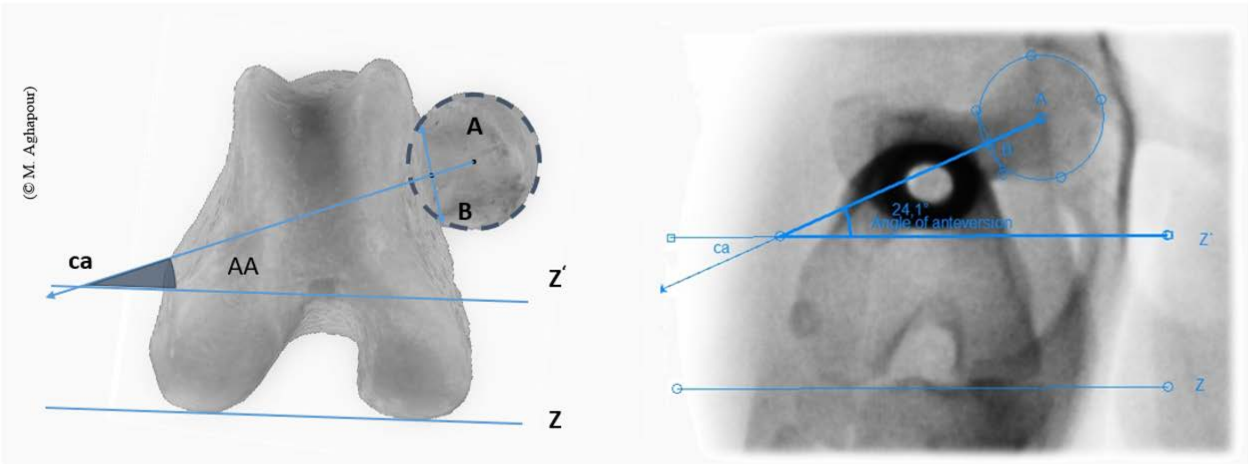

Figure 8. The angle of anteversion.

3.5.6 Anatomic caudal proximal femoral angle

Measurement of aCdPFA (Paley 2003, Yasukawa et al. 2016, Phetkaew et al. 2018) is shown in figure 9.

1. Use a circle to identify the center of the head of the femur so that it matches the outline of the bone in at least 3 points. The center of the circle is point **A.**

2. Identify the craniocaudal midpoint of the femoral neck at its narrowest point (**B**).
3. The axis of the femoral neck is represented by a straight line (**ca**) passing through points **A** and **B**.
4. To draw proximal anatomical axis (**paa**), we need to draw a reference line that is made from the proximal point of the lesser trochanter along the caudal cortex (**C**) to the proximal limit of the trochlea of the femur along the cranial cortex (**D**).
5. The line **CD** is divided into quarters and point **E** placed ¼ of the length of CD from proximal to distal.
6. **CE** is then divided into thirds.
7. The craniocaudal midpoint between the cortices is determined at ⅓ and ⅔ the length of the CE and marked as points (**F**) and (**G**) respectively (remain within the cortex).
8. The proximal anatomical axis (**paa**) is a straight line passing through points **F** and **G**.
9. The anatomic caudoproximal femoral angle (**aCdPFA**) is the angle between the axis of the neck of the femur (**ca**) and the proximal anatomic axis (**paa**).

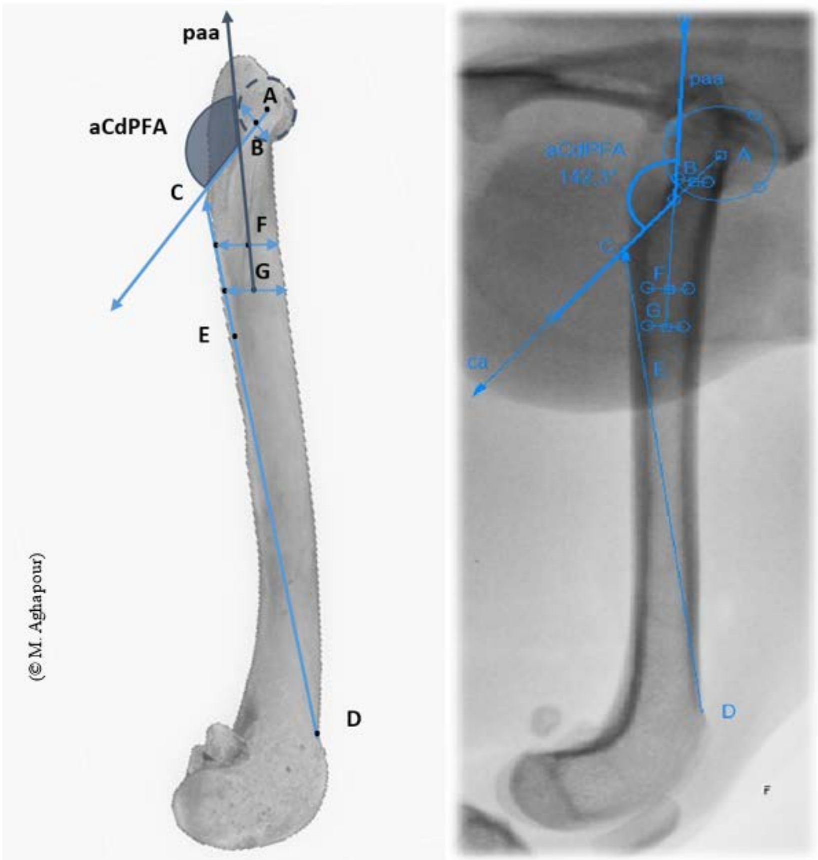

Figure 9. Anatomic caudal proximal femoral angle.

3.5.7 Anatomic caudal distal femoral angle

Measurement of aCdDFA (Paley 2003, Yasukawa et al. 2016, Phetkaew et al. 2018) is shown in figure 10.

1. To draw distal anatomical axis (**daa**), we need to draw a reference line that is made from the proximal point of the lesser trochanter along the caudal cortex (**C**) to the proximal limit of the trochlea of the femur along the cranial cortex (**D**).
2. This line **CD** is divided into quarters and point **H** placed ¼ of the length of CD from distal to proximal.
3. **HD** is then divided into thirds.
4. The craniocaudal midpoint between the cortices is determined at ⅓ and ⅔ the length of the HD and marked as points (**I**) and (**J**) respectively (remain within the cortex).
5. The proximal anatomical axis (**daa**) is a straight line passing through points (**I**) and (**J**).
6. Draw line (**X**) through the point (**D**) perpendicular to the reference line (**CD**).
7. The anatomic caudodistal femoral angle (**aCdDFA**) is the angle between the distal anatomic axis (**daa**) and the axis of the distal femur (**X**).

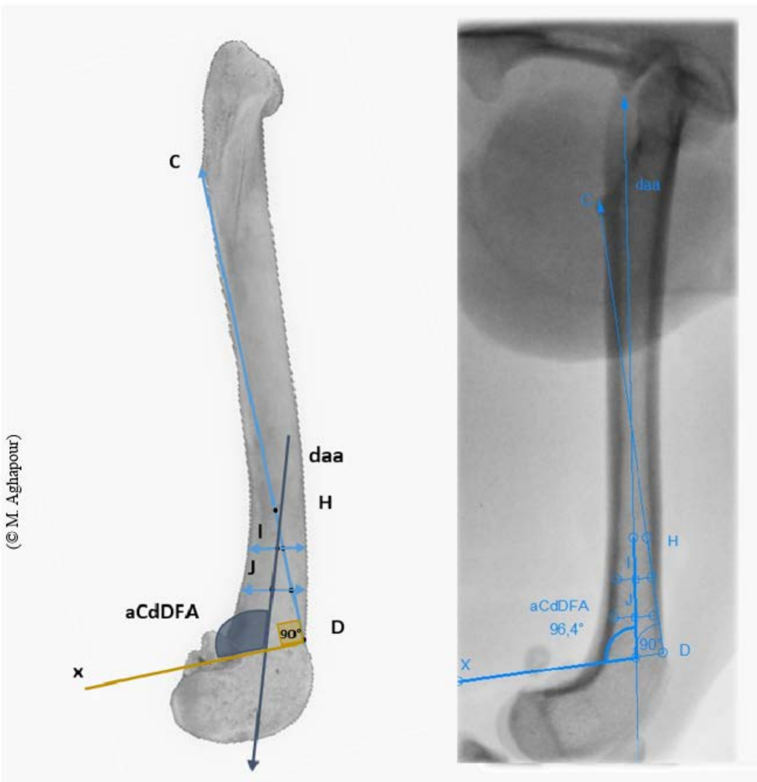

Figure 10. Anatomic caudal distal femoral angle.

3.5.8 Mechanical caudal proximal femoral angle

Measurement of mCdPFA (Paley 2003, Yasukawa et al. 2016) is shown in figure 11.

1. Use a circle to identify the center of the head of the femur so that it matches the outline of the bone in at least 3 points. The center of the circle is point **A.**
2. Identify the craniocaudal midpoint of the femoral neck at its narrowest point (**B**).
3. The axis of the femoral neck is represented by a straight line (**ca**) passing through points (**A**) and (**B**).
4. Mechanical axis defined by a straight line (**ma**) connecting the center of the proximal joint (**A**) with the center of the distal joint.
5. The mechanical caudoproximal femoral angle (**mCdPFA**) is the angle between the axis of the neck of the femur (**ca**) and the mechanical axis (**ma**).

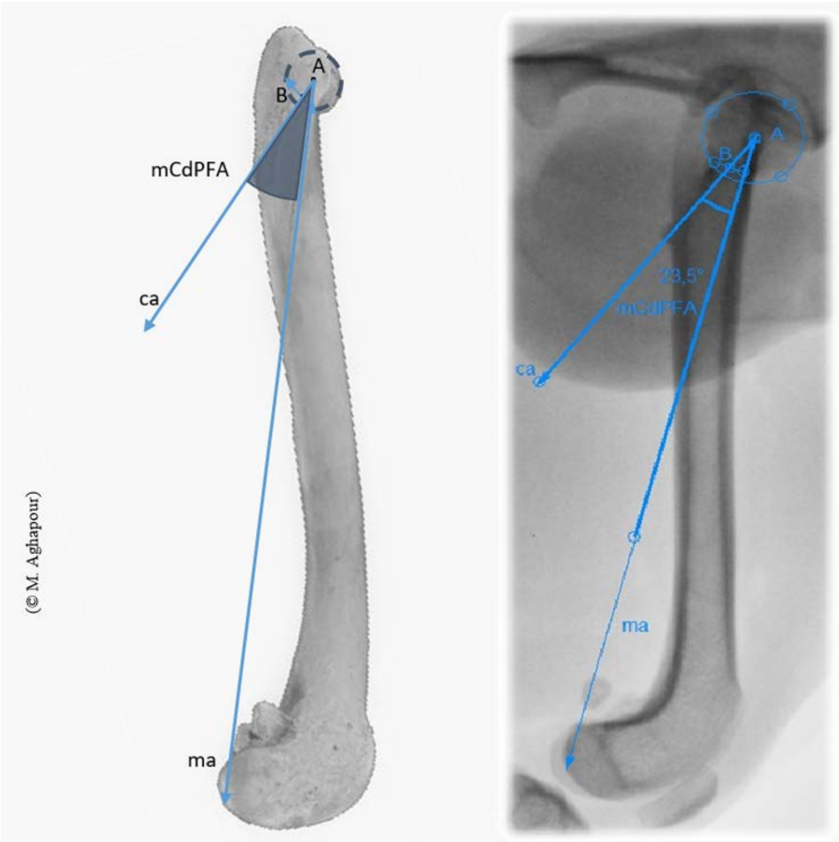

Figure 11. Mechanical caudal proximal femoral angle.

3.5.9 Mechanical caudal distal femoral angle

Measurement of mCdDFA (Paley 2003, Yasukawa et al. 2016) is shown in figure12.

1. Draw a reference line that is made from the proximal point of the lesser trochanter along the caudal cortex (**A**) to the proximal limit of the trochlea of the femur along the cranial cortex (**B**).
2. Draw Mechanical axis defined by a straight line (**ma**) connecting the center of the proximal joint with the center of the distal joint.
3. Draw line **X** through point **B** perpendicular to the reference line **AB.**
4. The mechanical caudodistal femoral angle (**mCdDFA**) is the angle between the axis of the distal femur (**X**) and the mechanical axis of the femur (**ma**).

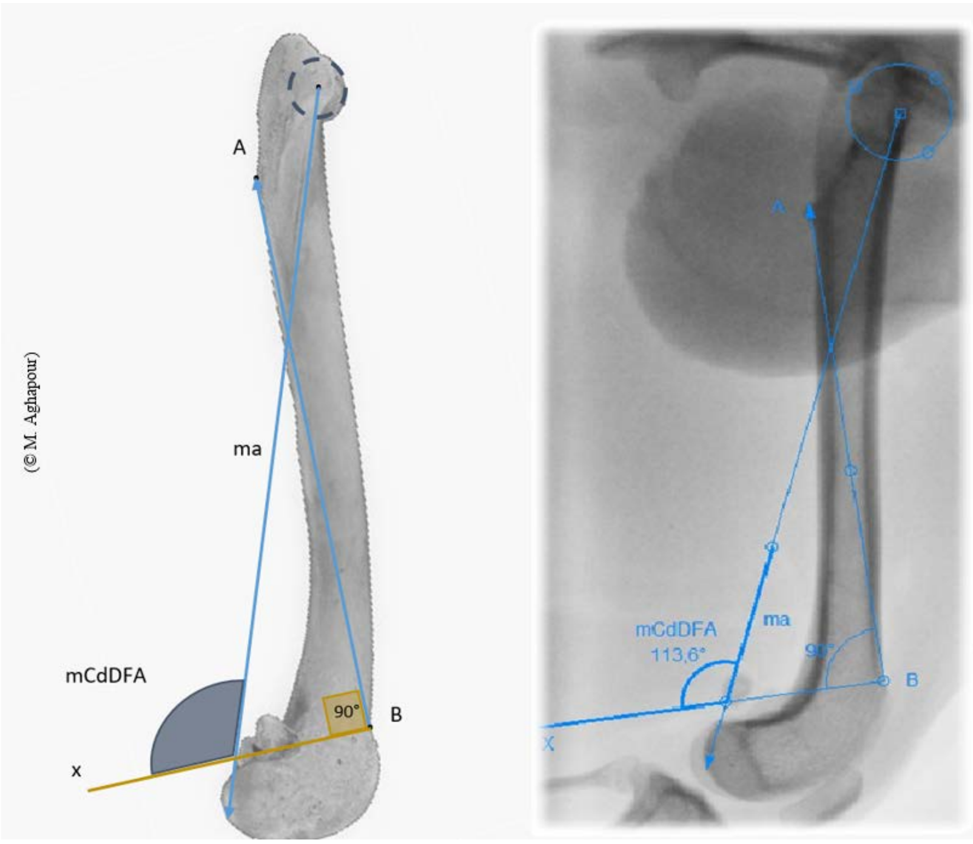

Figure 12. Mechanical caudal distal femoral angle.

3.5.10 Procurvatum angle

The procurvatum angle (PA) (Yasukawa et al. 2016, Phetkaew et al. 2018) is an angle between the proximal anatomical angle (**paa**) and distal anatomical angle (**daa**) in the sagittal plane, figure 13.

1. To draw the proximal anatomical axis **(paa)**, as described before :
   I. Draw a reference line that is made from the proximal point of the lesser trochanter along the caudal cortex (**A**) to the proximal limit of the trochlea of the femur along the cranial cortex (**B**).
   II. This line (**AB**) is divided into quarters and point (**C**) placed ¼ of the length of CD from proximal to distal.
   III. The (**AC**) is then divided into thirds and the craniocaudal midpoint between the cortices (remain within the cortex) is determined at ⅓ and ⅔ the length of the AC and marked as points (**E**) and (**F**)respectively.
   IV. The proximal anatomic axis (**paa**) is a straight line passing through points (**E**) and (**F**).
2. To draw distal anatomic axis **(daa)** as described before:
   I. Draw a reference line that is made from the proximal point of the lesser trochanter along the caudal cortex (**A**) to the proximal limit of the trochlea of the femur along the cranial cortex (**B**).
   II. This line (**AB**) is divided into quarters and point (**D**) placed ¼ of the length of CD from distal to proximal.
   III. (**DB**) is then divided into thirds. The craniocaudal midpoint (remain within the cortex) between the cortices is determined at ⅓ and ⅔ the length of the DB and marked as points (**G**) and (**H**) respectively.
   IV. The proximal anatomic axis (**daa**) is a straight line passing through points (**G**) and (**H**).
3. The procurvatum angle is the angle between the proximal anatomic axis (**paa**) and the distal anatomic axis (**daa**) in the sagittal plane.

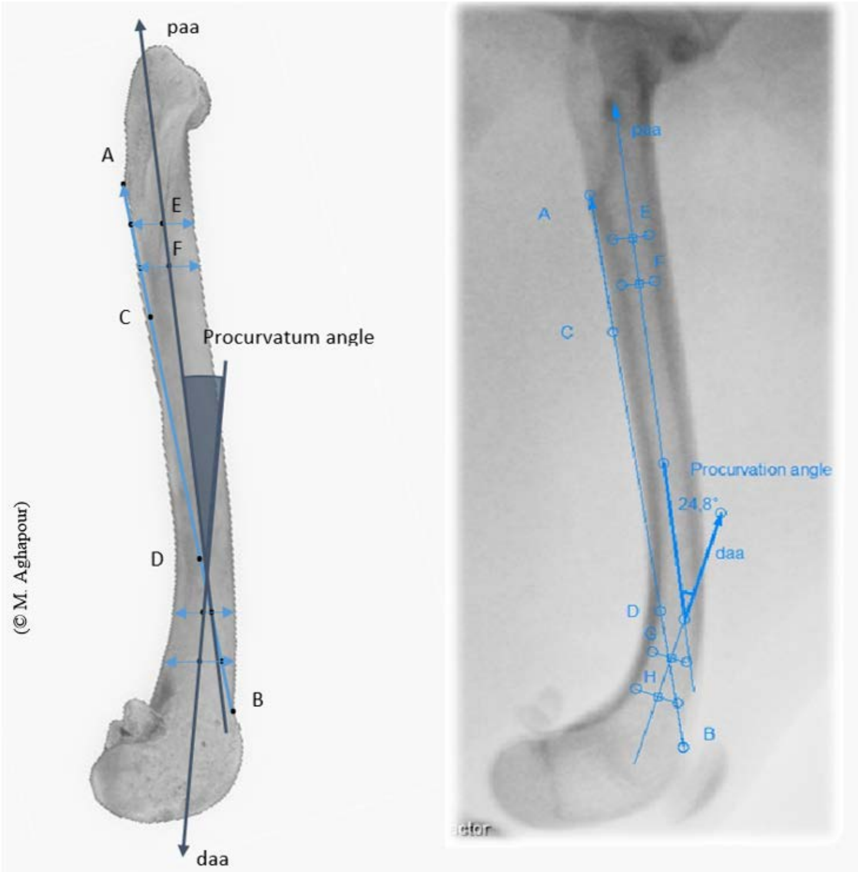

Figure 13. Procurvatum angle.

3.5.11 Mechanical medial proximal tibial angle and mechanical medial distal tibial angle

Measurements of mMPTA and mMDTA (Paley 2003, Dismukes et al. 2007) are shown in figure 14.

1. Draw the mechanical axis of tibia in frontal plane (**ma**), which is a straight line connecting the center of the proximal articular surface (midpoint between the two intercondylar tuberosities) (**A**) with the center of the distal articular surface (along the convexity of the caudal border of the cochlea of the tibia at the midpoint between medial and lateral malleoli) (**B**).
2. Draw the proximal joint orientation line in the frontal plane (**j**), which represented by a line passing through the distal points of the concavities of the medial and lateral tibial condyles.

3. Draw the distal joint orientation line in the frontal plane (**k**), which represented by a line passing through the proximal points of the medial and lateral concavities of the tibial cochlea.
4. Mechanical medial proximal tibial angle (**mMPTA**) is the angle between mechanical axis (**ma**) and proximal joint orientation line (**j**) in the medial side and mechanical medial distal tibial angle (**mMDTA**) is the angle between mechanical axis (**ma**) and distal joint orientation line (**k**) in medial side.

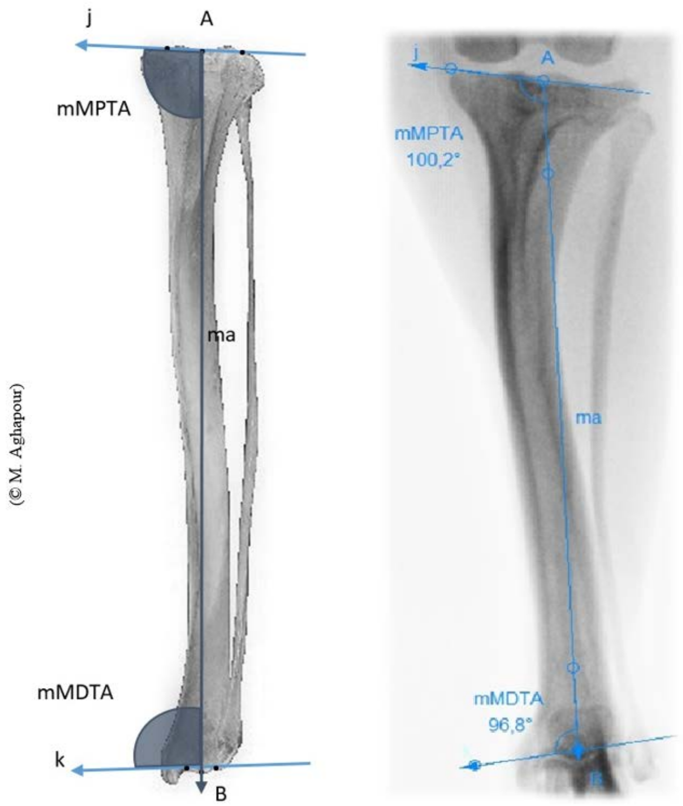

Figure 14. Mechanical medial proximal tibial angle and mechanical medial distal tibial angle.

3.5.12 Tibial plateau angle

Measurement of TPA (Dismukes et al. 2008b, Lambert and Wendelburg 2010, Glassman et al. 2011) is shown in figure15.

1. Draw the proximal joint orientation line (j) in the sagittal plane which is a line passing through the cranial and caudal extents of the tibial plateau.

2. Draw mechanical axis (ma) in the sagittal plane, which is represented by a straight line connecting the center of the proximal articular surface with the center of the distal articular surface (landmark: center of the talus).
3. Draw a perpendicular line (c) to the mechanical axis (ma) at the level of the intersection of the joint orientation line (j) and the mechanical axis (ma).
4. The Tibial plateau angle (TPA) is the angle between the proximal joint orientation line (j) and the Perpendicular line (c).

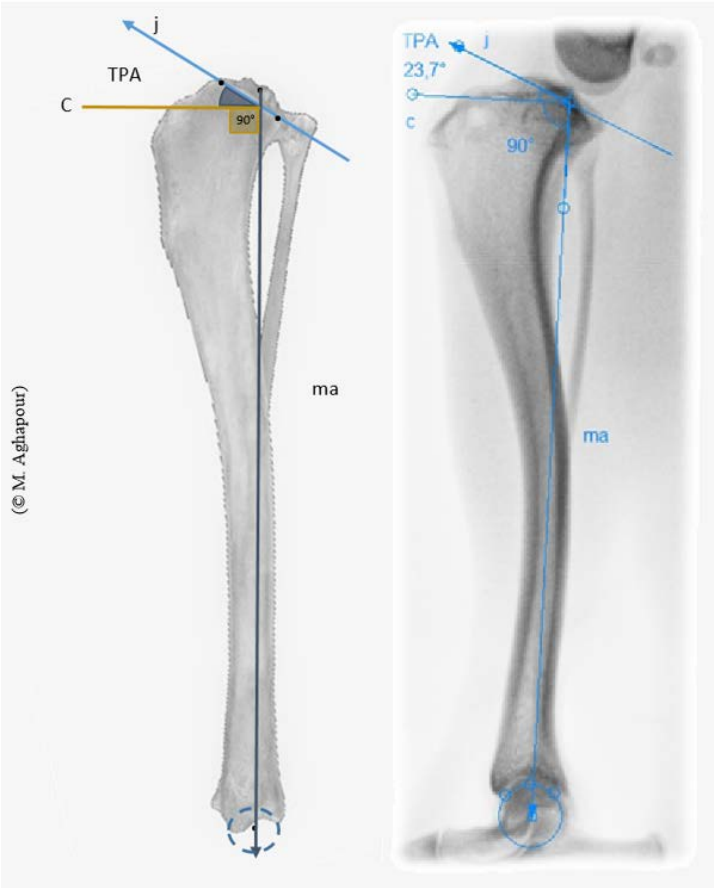

Figure 15. Tibial plateau angle.

3.5.13 Mechanical cranial proximal tibial angle, mechanical caudal proximal tibial angle, mechanical cranial distal tibial angle and mechanical caudal distal tibial angle

Measurements of mCrPTA, mCdPTA, mCrDTA and mCdDTA (Dismukes et al. 2008b) are shown in figure16.

1. Draw the proximal joint orientation line in the sagittal plane (**j**).

2. Draw mechanical axis (**ma**) in the sagittal plane, which is represented by a straight line connecting the center of the proximal articular surface with the center of the distal articular surface (landmark: center of the talus).
3. Draw the distal joint orientation line in the sagittal plane (**k**), which is a line connecting the most distal aspect of the cranial and caudal cortices of the tibia.
4. The angle between mechanical axis (**ma**) and joint orientation line (**j**) in proximal cranial part is the mechanical cranial proximal tibial angle (**mCrPTA**) and the angle between mechanical axis (**ma**) and joint orientation line (**j**) in proximal caudal part is the mechanical caudal proximal tibial angle (**mCdPTA**).
5. The angle between mechanical axis (**ma**) and joint orientation line (**k**) in distal cranial part is mechanical cranial distal tibial angle (**mCrDTA**) and the angle between mechanical axis (**ma**) and joint orientation line (**j**) in distal caudal part is the mechanical caudal distal tibial angle (**mCdDTA**).

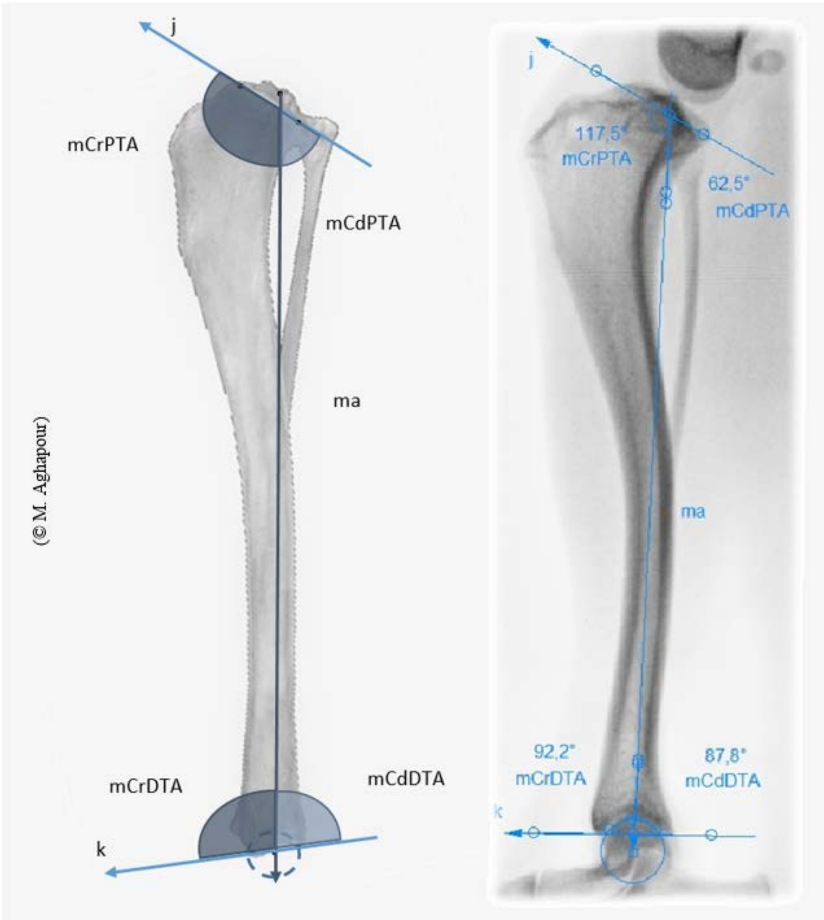

Figure 16. Mechanical cranial proximal tibial angle, mechanical caudal proximal tibial angle, mechanical cranial distal tibial angle and mechanical caudal distal tibial angle.

3.5.14 Z angle

Measurement of the Z angle (Vedrine et al. 2013, Aertsens et al. 2015) is shown in figure 17.

1. Draw mechanical axis (**ma**) in the sagittal plane, which is represented by a straight line connecting the center of the proximal articular surface with the center of the distal articular surface (landmark: center of the talus).
2. Draw line (**d**) which connecting the midpoint between the two tibial intercondylar tubercles with the most cranial point of the tibial tuberosity.
3. The **Z-angle** is the angle between the mechanical axis (**ma**) and the line (**d**).

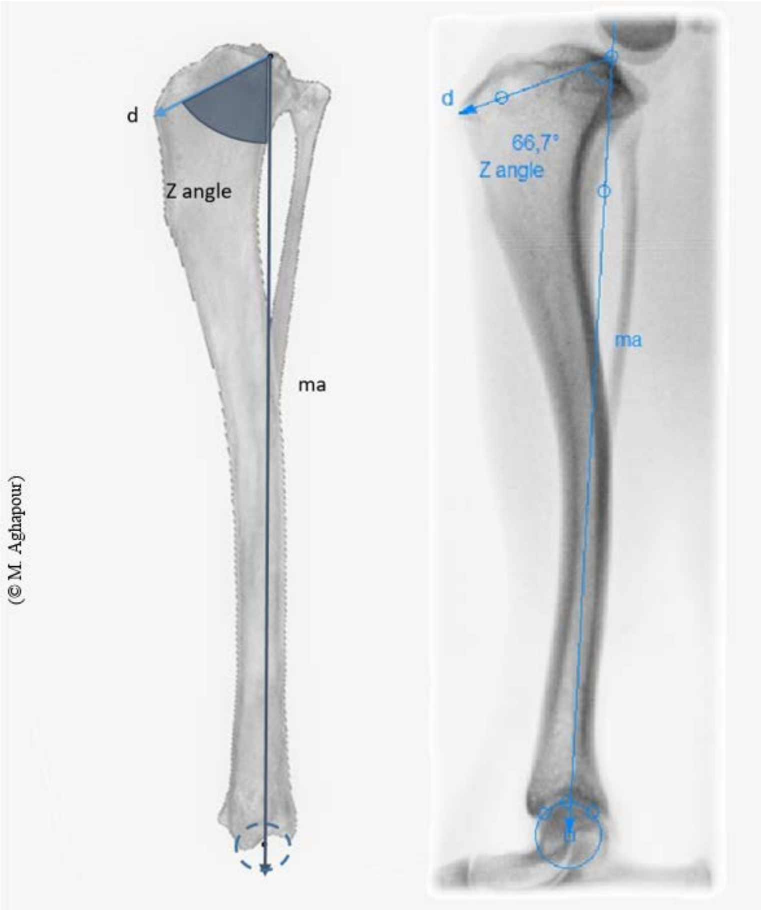

Figure 17. Z angle.

3.5.15 Proximal tibial axis inclination or distal tibial axis/proximal tibial axis angle or diaphyseal proximal tibial angle

Measurement of DPA (Osmond et al. 2006, Glassman et al. 2011) is shown in figure 18.

1. Measure the length of the tibia from the proximal point to the distal point in sagittal plane to identify the halfway down the length of the tibia and distal 1/3 of the length of the tibia.
2. Identify the midpoint of the craniocaudal cortices of the tibia in ½ (**A**) and distal ⅓ (**B**) of the length of the tibia (remain within the cortex) and draw a line which passes through point A and B (diaphyseal tibial axis).
3. Identify the distal aspect of the tibial crest point (**C**) and the cranial aspect of the medial tibial condyle point (**D**) and draw a perpendicular line from point C to the diaphyseal tibial axis.
4. Identify the craniocaudal midpoint between point **C** and diaphyseal tibial axis on the perpendicular line, Point (**E**).
5. Draw the proximal tibial axis (**PrA**), which is the line passing through the point (**D**) and (**E**).
6. The **DPA** (proximal tibial axis inclination) is the angle between (**PrA**) and diaphyseal tibial axis.

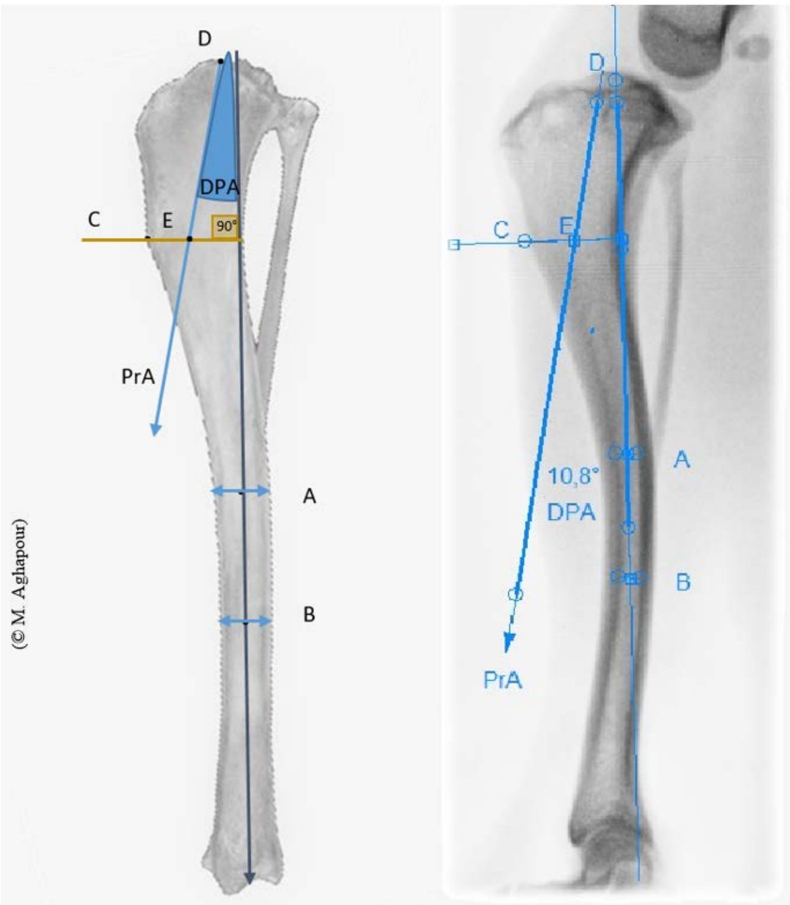

Figure 18. Proximal tibial axis inclination.

3.5.16 Relative tibial tuberosity width

Measurement of rTTW (Vedrine et al. 2013, Aertsens et al. 2015) is shown in figure 19.

1. Identify the most cranial point of the tibial plateau point (**A**), most caudal point of the tibial plateau point (**B**) and most proximal point of the margo cranialis tibiae point (**C**).
2. Draw a circle with the center of point **B** and radius of **AB**.
3. Draw (**BC**) line and identify the point (**D**) which is the cross point of the circle with the center (**B**) and the radius (**AB**) with the line (**BC**).
4. Measure the length of the line (**CD**) and (**DB**). The (**rTTW**) is defined by the ratio **CD/DB**.

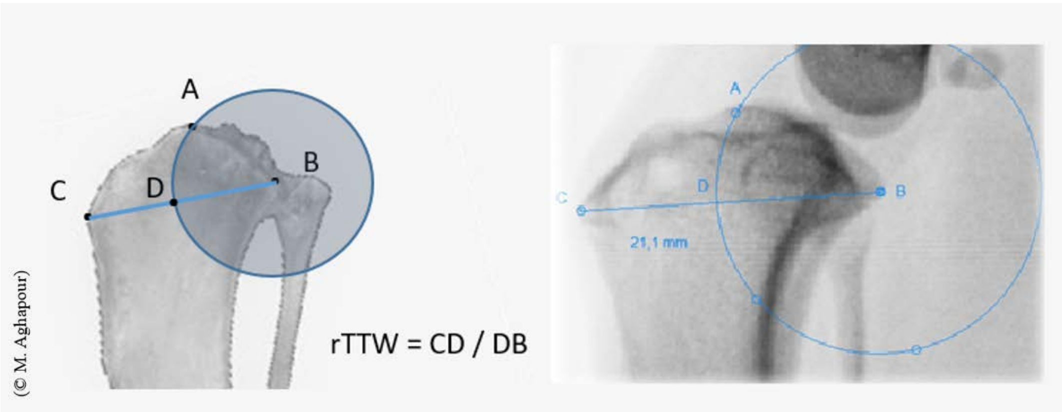

Figure 19. Relative tibial tuberosity width.

3.6 Study aims

3.6.1 **Category 1**: Studies that reported standard techniques and standard values

In 2005, Aper et al. evaluated tibial torsion using CT in the cadaveric specimen. One year later in 2006 Dudley et al. investigated femoral varus and torsion in sound dogs with CT and compared this technique with standard radiography and anatomic preparation. Osmond et al., 2006 investigated the morphology of the proximal tibia in dogs with and without CrCL rupture. Tomlinson et al., 2007 developed a standard method for measurement of femoral alignments in the frontal plane in four large breed dogs. Dismukes et al., 2007 described a standardized method for radiographic measurement of mMPTA and mMDTA in dogs with CrCL rupture. Later Dismukes et al. 2008a reported a standardized method for full-limb radiographic determination of hind limb alignments in the frontal plane. In another study Dismukes et al. 2008b described a method for determining mCdPTA and mCrDTA in Labrador Retrievers and non-Labrador Retrievers with CrCL disease. Mostafa et al., 2008 evaluated the proximodistal alignments of the patella in dogs. Later in 2010, Lambert and Wendelburg described anatomic landmarks for the measurement of mMPTA. The authors developed a tibia with varus deformity and evaluated the difference between tangential and straight caudocranial radiographic projection (tCdCr vs. sCdCr) before and after inducing a varus deformity. Łojszczyk-Szczepaniak et al. 2014 reported a reference range of Q angle in sound German shepherd dogs using radiographs. Sabanci and Ocal 2014 measured the lateral and medial TPA in sound dogs with radiographic and photographic methods. Witte 2015 assessed proximal tibial anatomy in healthy small breed dogs, to investigate optimal extracapsular stabilizing suture attachment sites and stifle joint angle and evaluated the influence of proximal tibial anatomy on these attachment site anisometry. In 2016, Hette et al. described a protocol for the measurement of torsion of the medial cortex of the tibia using CT. Savio et al. 2016 defined a new method for measurements of 3D morphometric parameters in polygonal mesh models of canine femora. Pinna and Romagnoli 2017 reported a reference value for Q angles in healthy dogs. Kara et al. 2018 investigated the correlation between the morphometric angles of the proximal and distal femora in sound dogs.

3.6.2 **Category 2**: Studies that compared the values in dogs with and without the different orthopedic diseases

In 2004 Sarierler compared the femoral inclination angle in dysplastic and non-dysplastic dogs using SYMAX (Rumph and Hathcock 1990) method. Mortari et al. 2009 assessed pre- and postoperative values of the Norberg angle, Q angle, FVA, and ICA in dogs with different grades of MPL. Ragetly et al. 2011 assessed conformation variables of the pelvic limbs of Labrador Retrievers that allow detection of limbs at risk to develop CrCL disease. Fitzpatrick et al. 2012 evaluated the influence of tibial torsion, age and sex on MPL in dogs with and without MPL using CT. Soparat et al. 2012 assessed femoral alignments of the Pomeranian dogs with and without MPL. Vedrine et al. 2013 investigated proximal tibia in healthy Labrador Retrievers and Yorkshire Terriers. Pinna et al. 2013 investigated the effect of intertrochanteric varus osteotomy on the Norberg angle and ICA in large breed dogs with early stage of hip dysplasia. Fuller et al. 2014 compared the tibial alignments in dogs with bilateral and unilateral CrCL rupture. In 2015, Aertsens et al. compared the TPA, Z angle, and rTTW between small and large dogs with CrCL disease. Su et al. 2015 compared TPA in small and large breed dogs with and without CrCL disease. In 2016, Hette et al. investigated the torsion of the medial cortex of the tibia in chondrodystrophic and non-chondrodystrophic dogs. Olimpo et al. 2016 investigated hind limb alignments of small breed dogs with and without MPL by radiographs. In the same year, Yasukawa et al. 2016 evaluated femoral, tibial and patellar alignments in Toy Poodles with and without MPL using radiography and CT. Guénégo et al. 2017 compared measurements of tibial alignments from radiographs of the predisposed dogs and dogs at low risk of CrCL rupture. Janovec et al. 2017 investigated proximal tibial alignments in small breed dogs with and without CrCL rupture. Lusetti et al. 2017 measured femoral and tibial alignments in English Bulldogs with and without MPL using CT. Newman and Voss 2017 evaluated femoral and tibial alignments in English Staffordshire Bull Terriers with and without congenital MPL using CT. Perry et al. 2017 evaluated the impact of femoral varus on postoperative complications and outcomes in dogs with different grades of MPL. In 2018 Garnoeva et al. evaluated the anatomic and mechanical femoral and tibial angles in small breed dogs with and without MPL. Phetkaew et al. 2018 evaluated the hind limb alignments in Chihuahuas with and without. Žilinčík et al. 2018 compared radiographic measurements of femoral alignments in Yorkshire Terriers with and without MPL.

3.6.3 **Category 3**: The studies that investigated the accuracy of measurement methods or tools

Aper et al. 2005 evaluated the tibial torsion in the cadaveric specimen using CT. Dudley et al. 2006 compared the measured femoral varus and torsion using CT, standard radiography and anatomic preparation. Osmond et al. 2006 investigated the morphology of the proximal portion of the tibia on the 3D model created with CT. Ginja et al. 2007 described a method for measurement of femoral neck anteversion angle in Estrela Mountain dogs with CT and compared the results with the standard radiographic biplanar method. Swiderski et al. 2008 evaluated radiographic and anatomic FVA in cadavers. Glassman et al. 2011 investigated inter- and intra-observer variability in radiographic measurement of TPA and DPA angle in dogs with CrCL rupture. Palmer et al. 2011 compared the measurement of aLDFA between radiographs and anatomic specimen across a broad range of varus conformation. Jackson & Wendelburg 2012 evaluated the effect of distal femoral elevation on radiographic measurements of aLDFA. In 2013, Oxley et al. assessed the precision of a novel protocol for the determination of FVA using. Mostafa et al. 2014 evaluated the measurement of FNA angle on single lateral radiographs and biplanar method and evaluated the correlation with AA from CT techniques in Labrador Retrievers with and without CrCL rupture. Barnes et al. 2015 evaluated the repeatability and reproducibility of measurements of aLDFA, AA, mMPTA, TTD and CTA using CT in dogs with and without MPL. Miles et al. 2015 evaluated the repeatability and reproducibility of four femoral axis methods for the measurement of aLDFA. Longo et al. 2018 investigated a novel 3D automated computer-aided method for computation of aLDFA, FNA, and FTA in cadavers of sound dogs and evaluated the repeatability and reproducibility of the protocols. Mostafa et al. 2018 evaluated the influence of traditional Reynolds technique has been used to assess femoral anteversion angle (t-FAA) and angled beam projection (a-FAA) methods on the measurements of femoral anteversion angle. The list of the included articles for each category is shown in table 4.

Table 4. Classification of the included articles in the study according to the study aims.

[1]Category 1	[2]Category 2	[3]Category 3
Aper et al. 2005	Sarierler 2004	Aper et al. 2005
Dudley et al. 2006	Mortari et al. 2009	Dudley et al. 2006
Osmond et al. 2006	Ragetly et al. 2011	Osmond et al. 2006
Tomlinson et al. 2007	Fitzpatrick et al. 2012	Ginja et al. 2007
Dismukes et al. 2007	Soparat et al. 2012	Swiderski et al. 2008
Dismukes et al. 2008a	Vedrine et al. 2013	Glassman et al. 2011
Dismukes et al. 2008b	Pinna et al. 2013	Palmer et al. 2011
Mostafa et al. 2008	Fuller et al. 2014	Jackson & Wendelburg 2012
Lambert and Wendelburg 2010	Aertsens et al. 2015	Oxley et al. 2013
Łojszczyk-Szczepaniak et al. 2014	Su et al. 2015	Mostafa et al. 2014
Sabanci and Ocal 2014	Hette et al. 2016	Barnes et al. 2015
Witte 2015	Olimpo et al. 2016	Miles et al. 2015
Hette et al. 2016	Yasukawa et al. 2016	Longo et al. 2018
Savio et al. 2016	Guénégo et al. 2017	Mostafa et al. 2018
Pinna and Romagnoli 2017	Janovec et al. 2017	
Kara et al. 2018	Lusetti et al. 2017	
	Newman and Voss 2017	
	Perry et al. 2017	
	Garnoeva et al. 2018	
	Phetkaew et al. 2018	
	Žilinčík et al. 2018	

[1]Category 1: Studies that reported standard techniques and standard values
[2]Category 2: Studies that compared the values in dogs with and without different orthopedic diseases
[3]Category 3: Studies that investigated the accuracy of measurement methods or tools

3.7 Femoral alignments in the frontal plane

3.7.1 Femoral inclination angle or femoral neck angle

The femoral inclination angle (ICA) transfers the biomechanical forces from the femur to the acetabulum. Different methods were developed for the measurements of the ICA. In 1979, Hauptman et al. reported two different methods for measurements of the ICA in dogs. There were no statistically different between age, breeds or sex of the dogs in this study. Radiographic positioning of the femur is important to achieve an accurate ICA, the true angle of inclination should be measured in the femur with 0° angle of anteversion (Hauptman et al. 1979), whereas 12° to 40° angle of anteversion has been reported for the normal femora (Nunamaker et al. 1973). Real ICA has been obtained by the trigonometric formula (Webber Formula No. 2). For example, in this study for a femur with 146° ICA and 27° Angle of anteversion, 142° real ICA was calculated (Hauptman et al. 1979). In 1985, Montavon et al. reported another method for correction of measured ICA and calculation of the real ICA. In 2004 Sarierler reported the values of ICA in dogs with and without hip dysplasia using SYMAX method. SYMAX method is a symmetric axis-based procedure developed by Rumph and Hathcock 1990. No significant difference between dysplastic and non-dysplastic dogs was recorded, thus significant difference was recorded between Doberman and Labrador, and between Anatolian Karabash and the other six breeds in this study. Tomlinson et al. 2007 reported that the Rottweilers had significantly higher ICA than German shepherds, Golden Retrievers and Labrador Retrievers, furthermore ICA of the Golden retrievers were significantly higher than German Shepherds in this study.

In 2009, Mortari et al. reported significantly lower postoperative ICA for the dogs with grades 2 and 3 MPL (lateral retinacular overlap and wedge recession sulcoplasty for the dogs with grade 2 MPL and lateral retinacular overlap wedge recession sulcoplasty, release of the quadriceps muscle and the tibial tuberosity transposition for the dogs with grade 3 MPL) in compare with pre-operative values. Soparat et al. 2012 found no significant difference for ICA in Pomeranians with and without MPL. Pinna et al. 2013 investigated the effect of intertrochanteric varus osteotomy on hind limb alignments including ICA in large breed dogs with early stage of hip dysplasia and reported a significantly decreased postoperative ICA when compared to the preoperative ICA. Savio et al. 2016 reported standard values of ICA in sound dogs using radiography, 3D models and projected planes. Olimpo et al. 2016 reported no significant difference for measured ICA between healthy small breed dogs and dogs with different grades of MPL, which confirmed the results reported for Pomeranian dogs in 2012. The same results reported by Yasukawa et al. 2016 for Toy Poodles, Lusetti et al. 2017 for English Bulldogs and Newman and Voss 2017 for English Staffordshire Bull Terriers with and without MPL. The results reported by Perry et al. 2017 for ICA, were correlated with previous studies as well. In another study, Garnoeva et al. 2018 reported that higher ICA was recorded for the dogs with grades 2 and 3 MPL in comparison with healthy dogs, which was contrary to the previous studies. No correlation was reported by Kara et al. 2018 between ICA and aLDFA or aCdDFA in normal canine femora. Longo et al. 2018 measured the ICA using radiography, CT and three-dimensional automated computer-aided design (CAD) and reported the values for each method. Repeatability and reproducibility of the CAD method were higher than radiography and CT in this study. Phetkaew et al. 2018 concluded that there was no difference between ICA of the Chihuahuas with and without MPL with both radiography and CT methods, suggesting no association between MPL and coxa vara. The study performed by Žilinčík et al. 2018 was confirmed the results of the previous studies as well. The values reported for ICA in the included articles are shown in table 5.

Table 5. Mean ± standard deviation of the ICA reported in the literature.

<table>
<tr><th>Author</th><th>ICA (°)</th><th>Author</th><th>ICA (°)</th></tr>
<tr><td>Hauptman et al. 1979</td><td>Method A: 146.2 ± 4.8
Method B: 129.4 ± 4.9</td><td>Yasukawa et al. 2016</td><td>Healthy: [3]Radio: 127.7 ± 6.3, [4]CT: 116.8 ± 6.1
MPL 2: Radio: 124.6 ± 7.1, CT: 118.0 ± 6.8
MPL 4: Radio: 125.0 ± 6.1, CT: 118.3 ± 9.3</td></tr>
<tr><td>Montavon et al. 1985</td><td>148.8 ± 3.7</td><td>Lusetti et al. 2017</td><td>Healthy: 129.11 ± 8.03
MPL: 124.53 ± 8.30</td></tr>
<tr><td>[1] Sarierler 2004</td><td>German Shepherd: 129.9 ± 0.46
Labrador Retriever: 131.61 ± 0.76
Pointer: 129.84 ± 0.98
Irish Setter: 128.91 ± 1.51
Anatolian Karabash: 138.60 ± 1.29
Doberman Pinscher: 127.04 ± 1.07
Golden Retriever: 129.25 ± 2.75</td><td>Newman & Voss 2017</td><td>Limbs from unaffected dogs: 136.72 ± 8.27
affected limbs: 135.35 ± 7.08</td></tr>
<tr><td>Tomlinson et al. 2007</td><td>Labrador retriever: 134 ± 5.3
Golden Retriever: 134 ± 5.2
German Shepherd: 132 ± 5.9
Rottweiler: 137 ± 5.4</td><td>[5] Perry et al. 2017</td><td>MPL 1: 131.2 [127.3 – 1 35]
MPL 2: 132.6 [120.9 – 1 57.8]
MPL 3: 136.4 [116.5 – 1 63.2]
MPL 4: 134.6 [126.5 – 149.5]</td></tr>
<tr><td>[2] Mortari et al. 2009</td><td>MPL 1: 131.2 ± 5.3
MPL 2: 130.4 ± 9.5
MPL 3: 133.8 ± 12
MPL 4: 136.7 ± 4.3</td><td>[5] Garnoeva et al. 2018</td><td>Healthy: 129 [117–146]
MPL 1: 130 [113–148]
MPL 2: 132 [119–168]
MPL 3: 138 [110–150]</td></tr>
<tr><td>Soparat et al. 2012</td><td>Healthy: 136.46 ± 7.12
MPL 1 -2: 136.76 ± 6
MPL 3: 139 ± 9</td><td>[1]Kara et al. 2018</td><td>146.24 ± 5.49</td></tr>
<tr><td>Pinna et al. 2013</td><td>Pre-Operative: 127.6 ± 2.6
Post-Operative: 111.3 ± 4.6</td><td>[6] Longo et al. 2018</td><td>Radio: 125.06 ± 5.4
CT: 125.80 ± 6.1
[7]CAD: 128.78 ± 4.2</td></tr>
<tr><td>Savio et al. 2016</td><td>Radio: 120.2 ± 8.0
Projected planes: 132.1 ± 3.5
3D model: 129.6 ± 4.3</td><td>Phetkaew et al. 2018</td><td><table>
<tr><th></th><th colspan="2">Radio</th><th rowspan="2">CT</th></tr>
<tr><th></th><th>[8]CrCd</th><th>[9]CdCr</th></tr>
<tr><td>Healthy</td><td>133.2 ± 7.9</td><td>131.3 ± 3.6</td><td>130.9 ± 4.4</td></tr>
<tr><td>MPL 1</td><td>134.1 ± 3.5</td><td>134.0 ± 5.8</td><td>134.6 ± 7.0</td></tr>
<tr><td>MPL 2</td><td>132.5 ± 4.4</td><td>134.7 ± 6.4</td><td>133.4 ± 5.2</td></tr>
<tr><td>MPL 3</td><td>135.2 ± 8.4</td><td>132.8 ± 7.9</td><td>133.7 ± 4.9</td></tr>
<tr><td>MPL 4</td><td>141.7 ± 7.6</td><td>137.5 ± 8.6</td><td>129.5 ± 6.9</td></tr>
</table></td></tr>
<tr><td>Olimpo et al. 2016</td><td>Healthy: 130 ± 6.5
MPL 1: 127.23 ± 3.3
MPL 2: 125.3 ± 4.7
MPL 3: 130.4 ± 6.2
MPL 4: 130 ± 3.5</td><td>Žilinčík et al. 2018</td><td>Healthy: 125.39 ± 4.13
MPL 1: 125.07 ± 3.67
MPL 2: 123.82 ± 7.01
MPL 3: 126.50 ± 4.13
MPL 4: 127.04 ± 4.22</td></tr>
</table>

[1] Values for Healthy dogs
[2] Pre-operative values
[3] Radiography
[4] Computed Tomography
[5] Results are reported as median [minimum-maximum]
[6] Average of three observers for normal femora
[7] three-dimensional automated computer-aided design
[8] Craniocaudal
[9] Caudocranial

3.7.2 Anatomic lateral proximal femoral angle and mechanical lateral proximal femoral angle

The importance of aLPFA and mLPFA angles is to evaluate the anatomic structure of the proximal femur especially in the case of fracture and to assess the fracture healing process (Tomlinson et al. 2007). Different studies reported values for aLPFA, mLPFA in sound dogs or dogs with different orthopedic diseases. Tomlinson et al. 2007 reported a significant difference between the shape of the greater trochanter and femoral head among Labrador Retrievers, Golden Retrievers, German Shepherds, and Rottweilers. Labrador Retrievers had significantly higher aLPFA and mLPFA values than the other three dog breeds in this study; however, German shepherds had significantly higher aLPFA and mLPFA values than Golden Retrievers and Rottweilers. No significant difference was reported for mLPFA for the Golden Retrievers and Rottweilers in this study. The radiographic positioning of the dogs is an important factor to achieve accurate measurements. Radiographs are susceptible to positioning error (Swiderski et al. 2008, Barnes et al. 2015) and the risk of positioning error raises in dogs with bone deformities, such as severe grades of patellar luxation (Mortari et al. 2009). The radiographic positioning of the femur can influence the relative position of the greater trochanter, which is an important landmark to draw the proximal joint orientation line in the femur (Tomlinson et al. 2007). In a study on dogs with CrCL disease Dismukes et al. 2008a, reported a significantly higher mLPFA for female dogs compared with male dogs.

In 2016 Savio et al. defined a new method for measurement of 3D morphometric parameters of the femur in sound dogs. Measurements were performed on radiographs and 3D models, which were obtained by a 3D scanner, however, another round of measurements were performed on femora inclined at an angle of 25° with a caudal-cranial orientation to simulate the positioning of the femur during hip extension. The authors reported that the 3D method minimizes the variability of the measurements related to the observer or positioning of the dog. The measured angles with the 3D method were different from those measured with the radiographic method due to the different femoral axes. Olimpo et al. 2016 in a radiographic study, reported no significant difference for aLPFA and mLPFA between healthy dogs and dogs with different grades of MPL. Yasukawa et al. 2016 reported the same results with radiography and CT between healthy dogs and dogs with grades 2 and 4 MPL. No significant difference was reported from Lusetti et al. 2017 for aLPFA and mLPFA between the purebred English Bulldogs with and without MPL using the CT method. In 2018 Garnoeva et al. confirmed the previous results reported by Olimpo et al. 2016, Yasukawa et al. 2016, Lusetti et al. 2017 and reported no significant difference for aLPFA and mLPFA between sound dogs and dogs with MPL, Whereas Phetkaew et al. 2018 reported a significant difference for aLPFA and mLPFA values between CT scan images and radiographic images in craniocaudal and caudocranial radiographs in healthy Chihuahuas. Žilinčík et al. 2018 reported that the mean values for aLPFA in the Yorkshire terriers with grade 4 MPL were significantly less than those in other groups. The values reported for aLPFA and mLPFA in the included articles are shown in table 6.

Table 6. Mean ± standard deviation of the aLPFA and mLPFA reported in the literature.

<table>
<tr><th>Author</th><th colspan="4">aLPFA (°)</th><th colspan="4">mLPFA (°)</th></tr>
<tr><td>Tomlinson et al. 2007</td><td colspan="4">Labrador retriever: 103 ± 6.4
Golden Retriever: 98 ± 5.7
German Shepherd: 101 ± 5.0
Rottweiler: 96 ± 5.3</td><td colspan="4">Labrador retriever: 100 ± 6.0
Golden Retriever: 95 ± 5.2
German Shepherd: 97 ± 4.5
Rottweiler: 93 ± 4.7</td></tr>
<tr><td>Dismukes et al. 2008a</td><td colspan="4"></td><td colspan="4">103.7 ± 5.4</td></tr>
<tr><td>Savio et al. 2016</td><td colspan="4">[1]Radio: 109.6 ± 5.9
[2]Projected planes: 103.7 ± 5.9
3D model: 115.2 ± 3.9</td><td colspan="4">Radio: 105.3 ± 5.2
Projected planes: 98.4 ± 5.3
3D model: 105.5 ± 4.2</td></tr>
<tr><td>Olimpo et al. 2016</td><td colspan="4">Healthy: 114.9 ± 8.6
MPL 1: 114 ± 9.1
MPL 2: 109.7 ± 8
MPL 3: 110.6 ± 8.2
MPL 4: 98.3 ± 0</td><td colspan="4">Healthy: 105.1 ± 4.6
MPL 1: 107.6 ± 7.7
MPL 2: 104.6 ± 7.7
MPL 3: 106 ± 7.6
MPL 4: 93.6 ± 0.5</td></tr>
<tr><td rowspan="3">Yasukawa et al. 2016</td><td></td><td>Healthy</td><td>MPL 2</td><td>MPL 4</td><td></td><td>Healthy</td><td>MPL 2</td><td>MPL 4</td></tr>
<tr><td>Radio</td><td>106.6 ± 8.7</td><td>107.6 ± 6.3</td><td>96.5 ± 8.4</td><td>Radio</td><td>102.1 ± 8.8</td><td>101.5 ± 7.7</td><td>93.8 ± 5.5</td></tr>
<tr><td>CT</td><td>119.5 ± 5.7</td><td>118.7 ± 4.4</td><td>112.7 ± 6.8</td><td>CT</td><td>113.6 ± 6.1</td><td>113.1 ± 3.9</td><td>109.7 ± 6.4</td></tr>
<tr><td>Lusetti et al. 2017</td><td colspan="4">Healthy: 111.75 ± 6.66
MPL: 112.21 ± 9.29</td><td colspan="4">Healthy: 111.02 ± 6.90
MPL: 108.12 ± 7.75</td></tr>
<tr><td>[3] Garnoeva et al. 2018</td><td colspan="4">Healthy: 110 [94–128]
MPL 1: 106.5 [99–114]
MPL 2: 109 [91–129]
MPL 3: 111 [93–126]</td><td colspan="4">Healthy: 107 [90–127]
MPL 1: 106 [100–116]
MPL 2: 108 [71–173]
MPL 3: 111 [94–130]</td></tr>
<tr><td rowspan="7">Phetkaew et al. 2018</td><td rowspan="2"></td><td colspan="2">Radio</td><td rowspan="2">CT</td><td rowspan="2"></td><td colspan="2">Radio</td><td rowspan="2">CT</td></tr>
<tr><td>[4]CrCd</td><td>[5]CdCr</td><td>CrCd</td><td>CdCr</td></tr>
<tr><td>Healthy</td><td>113.0 ± 4.2</td><td>112.7 ± 7.6</td><td>124.2 ± 6.6</td><td>Healthy</td><td>109.9 ± 7.9</td><td>108.5 ± 8.2</td><td>120.0 ± 7.1</td></tr>
<tr><td>MPL 1</td><td>111.2 ± 6.2</td><td>108.8 ± 5.4</td><td>120.5 ± 4.4</td><td>MPL 1</td><td>109.0 ± 7.3</td><td>105.2 ± 5.9</td><td>117.0 ± 5.8</td></tr>
<tr><td>MPL 2</td><td>115.9 ± 7.7</td><td>110.3 ± 8.6</td><td>122.4 ± 7.3</td><td>MPL 2</td><td>112.6 ± 8.3</td><td>107.3 ± 8.6</td><td>120.5 ± 8.6</td></tr>
<tr><td>MPL 3</td><td>113.8 ± 8.3</td><td>110.5 ± 9.7</td><td>122.5 ± 7.1</td><td>MPL 3</td><td>113.4 ± 8.1</td><td>107.8 ± 9.4</td><td>118.9 ± 8.4</td></tr>
<tr><td>MPL 4</td><td>108.5 ± 11.7</td><td>103.8 ± 16.4</td><td>125.2 ± 7.5</td><td>MPL 4</td><td>109.6 ± 9.1</td><td>104.2 ± 11.4</td><td>122.8 ± 7.1</td></tr>
<tr><td>Žilinčík et al. 2018</td><td colspan="4">Healthy: 118.58 ± 3.40
MPL 1: 120.47 ± 1.87
MPL 2: 118.22 ± 6.54
MPL 3: 119.63 ± 3.59
MPL 4: 94.74 ± 4.98</td><td colspan="4">n/a</td></tr>
</table>

[1]Radio: Radiography
[2]Projected plane with the femur inclined at an angle of 25° with a caudal-cranial orientation
[3]The results are reported as median [minimum-maximum] in this study
[4]CrCd: craniocaudal projection
[5]CdCr: caudocranial projection
n/a: not provided

3.7.3 Anatomic lateral distal femoral angle, mechanical lateral distal femoral angles, and femoral varus angle

Distal femoral angles including aLDFA, mLDFA, and FVA are important alignments to evaluate the distal femoral deformities. The incidence of varus or valgus deformities in the distal part of the femur is greater than those in proximal femur (Hulse 1993, Tomlinson et al. 2007), these deformities may be one of the predisposing's of the patellar luxation in dogs but the exact amount of the femoral distal varus or valgus that cause MPL or LPL is unknown (Tomlinson et al. 2007). In 2006, Dudley et al. described a CT technique for the determination of the femoral varus angle in sound dogs and compared this technique with standard radiography and anatomic preparation. No difference was reported between the three methods. Tomlinson et al. 2007 reported no significantly different aLDFA and mLDFA between Labrador Retriever, Golden Retriever, and Rottweiler dogs but German Shepherds had significantly lower values than the other three large breeds. Dismukes et al. 2008a reported no significant difference for mLDFA between male and female dogs, right and left limb and tarsal valgus and varus deformities in dogs with CrCL rupture. Swiderski et al. 2008 evaluated radiographic and anatomic FVA in sound cadavers. Intra- and inter-observer variance of radiographic measurements were acceptable in this study but not statistically accurate in predicting anatomic FVA. No significant difference between the radiographic and anatomic measurements was found in this study. Palmer et al. 2011 compared the measurement of aLDFA between radiographs and anatomic specimen with and without wedges on distal femurs. An acceptable intra- and inter-observer agreement was recorded for radiographic aLDFA and femoral specimen's aLDFA. The authors concluded that the radiographic measurement of the aLDFA did not reach the desired accuracy for the measurement of the femoral varus. Jackson and Wendelburg 2012 assessed the effect of distal femoral elevation on radiographic measurements of aLDFA. Seven cadavers of medium-large breed dogs without orthopedic disorders were evaluated. The results showed a significant increase in measured aLDFA at all elevations above 5° when compared to 0° elevation. Soparat et al. 2012 reported a significantly greater aLDFA, mLDFA and FVA for the Pomeranians with grade 3 MPL in comparison with grades 1 and 2 MPL and healthy Pomeranians. Oxley et al. 2013 reported high intra- and inter-observer ICCs for measured FVA with CT in this study. As a result of femoral rotational and sagittal plane malpositioning, consistent linear variations were seen in measured FVA. The authors concluded that a small amount of positioning error, which is not unexpected during the positioning of the femur, may cause statically significant error in the measurement of FVA. Barnes et al. 2015 reported a good intra- and inter-observer agreement for measured aLDFA with CT in dogs with and without MPL. Most of the variance in the measurement of each parameter in this study was attributable to the dog. Miles et al. 2015 evaluated the intra- and inter-observer variability of four different measurement methods of aLDFA by radiographs and investigated aLDFA agreement between and within these methods for the femora at 0°, 12.5°, and 25° elevations. Small intra- and inter-observer differences were recorded between the methods in this study. High ICCs (intra-class correlation coefficient) were recorded for all methods; however, the median aLDFA increased significantly with increasing femoral elevation for all methods. Savio et al. 2016 reported values for FVA using radiography, 3D models and projected planes. Olimpo et al. 2016 reported a significantly higher aLDFA for small breed dogs with grade 4 MPL compared to the healthy dogs and other grades of MPL. Yasukawa et al. 2016 reported significantly greater aLDFA, mLDFA, and FVA values for Toy Poodles with grade 4 MPL on radiographs and CT scans. The same results reported by Lusetti et al. 2017 for aLDFA and mLDFA in English Bulldogs with MPL compared to the healthy English Bulldogs. FVA was not evaluated in this study. The study performed by Newman and Voss 2017 confirmed the results of previous studies for aLDFA and reported increased values of aLDFA in English Staffordshire Bull Terriers with MPL, but this increase was not statistically significant in this study. Perry et al. 2017 evaluated the postoperative outcome of the dogs with MPL that undergone a surgical correction. Very good inter-observer variabilities were recorded for the measurements of aLDFA, mLDFA, and FVA between three observers in this study. Garnoeva et al. 2018 confirmed former results reported for aLDFA, mLDFA, and FVA in dogs with MPL and reported significantly lower values for mentioned angles in healthy small breed dogs compared to the grades 1,2 and 3 MPL. Kara et al. 2018 reported a weak positive correlation between the AA and aLDFA. No evidence of a sex difference in the aLDFA measurements was found in this study. Longo et al. 2018 reported that the aLDFA was the most repeatable and reproducible angle with excellent ICCs for all radiography, CT imaging, and three-dimensional automated computer-aided design methods. Phetkaew et al. 2018 defined that based on CT scans the mLDFA was related to the severity of MPL in Chihuahuas and it was significantly increased in dogs with grades 3 and 4 MPL. The aLDFA was significantly increased in dogs with grade 3 MPL as well, furthermore, no significant differences between radiographic and CT imaging methods were reported for aLPFA and mLPFA in sound stifles. The results of the study performed by Žilinčík et al. 2018 corresponded with the previous studies. The authors reported significantly greater aLDFA and FVA for the Yorkshire Terriers with grade 4 MPL in comparison with other grades of MPL and healthy Yorkshire Terriers. The values reported for the aLDFA, mLDFA, and FVA are shown in table 7 for the healthy dogs and in table 8 for the dogs with medial patellar luxation.

Table 7. Mean ± standard deviation of the aLDFA, mLDFA, and FVA in healthy dogs.

Dog Breeds	aLDFA° [Author]	mLDFA° [Author]	FVA° [Author]
Small breeds	95.0 ± 3.5 [Olimpo et al., 2016] Rad 96 [75–114] [Garnoeva et al., 2018] Rad *	103.1 ± 3.4 [Olimpo et al., 2016] Rad 100 [84–116] [Garnoeva et al., 2018] Rad *	5.5 [3–23] [Garnoeva et al., 2018] Rad*
Medium to large breed	92.32 ± 2.46 [Jackson & Wendelburg,2012] Rad 95.04 ± 3.35 [Jackson & Wendelburg,2012] Rad+ 92.6 ± 3.8 [Savio et al., 2016] Rad 88.6 ± 4.5 [Savio et al., 2016] 3D 91.06 ± 4.54 [Longo et al., 2018] ** 91.38 ± 4.44 [Longo et al., 2018] CT	96.9 ± 2.9 [Savio et al., 2016] Rad 93.4 ± 3.9 [Savio et al., 2016] 3D	9.4 ± 2.3 [Dudley et al., 2006] Rad 8.8 ± 3.3 [Dudley et al., 2006] CT 7.4 ± 3.9 [Dudley et al., 2006] Ana 5.8 ± 1.0 [Swiderski et al., 2008] Rad 5.2 ± 2.1 [Swiderski et al., 2008] Ana 2.6 ± 3.8 [Savio et al., 2016] Rad -1.4 ± 4.5 [Savio et al., 2016] 3D
Large breed	92.0° – 96.4° (4.4°) [Palmer et al., 2011] Rad ***	n/a	n/a
Different breeds	93.35 ± 3.16 [Kara et al., 2018] CT	n/a	n/a
Labrador retriever	97 ± 3.2 [Tomlinson et al., 2007] Rad	100 ± 2.6 [Tomlinson et al., 2007] Rad	n/a
Golden Retriever	97 ± 2.8 [Tomlinson et al., 2007] Rad	100 ± 2.3 [Tomlinson et al., 2007] Rad	n/a
German Shepherd	94 ± 3.3 [Tomlinson et al., 2007] Rad	97 ± 3.1 [Tomlinson et al., 2007] Rad	n/a
Rottweiler	98 ± 3.5 [Tomlinson et al., 2007] Rad	100 ± 2.7 [Tomlinson et al., 2007] Rad	n/a
Pomeranian	95.21 ± 3.48 [Soparat et al., 2012] Rad	99.46 ± 4 [Soparat et al., 2012] Rad	5.85 ± 3.18 [Soparat et al., 2012] Rad
Toy Poodles	94.4 ± 4.1 [Yasukawa et al., 2016] Rad 90.3 ± 2.8 [Yasukawa et al., 2016] CT	99.1 ± 3.1 [Yasukawa et al., 2016] Rad 96.2 ± 2.5 [Yasukawa et al., 2016] CT	4.4 ± 4.1 [Yasukawa et al., 2016] Rad 0.3 ± 2.8 [Yasukawa et al., 2016] CT
English Bulldogs	92.33 ± 4.75 [Lusetti et al., 2017] CT	101.56 ± 2.73 [Lusetti et al., 2017] CT	n/a
English Staffordshire Bull Terriers	96.18 ± 4.06 [Newman and Voss 2017] CT	n/a	n/a
Chihuahuas	101.2±4.8 [Phetkaew et al., 2018] Rad CrCd 97.1±3.8 [Phetkaew et al., 2018] Rad CdCr 95.7±3.6 [Phetkaew et al., 2018] CT	102.6±3.1 [Phetkaew et al., 2018] Rad CrCd 101.6±3.2 [Phetkaew et al., 2018] Rad CdCr 99.9±3.6 [Phetkaew et al., 2018] CT	n/a
Yorkshire Terriers	95.63 ± 2.14 [Žilinčík et al., 2018] Rad	n/a	5.63 ± 2.11 [Žilinčík et al., 2018] Rad

* Results are reported as median [minimum-maximum] in these studies
**Average of three observers for normal femora
*** Values are reported as min-max (range) in this study for healthy anatomic specimen
+ Radiograph in 45° elevation
3D: Three-dimensional measurements
Ana: Anatomic specimen
CdCr: Caudocranial projection
CrCd: Craniocaudal projection
CT: Computed Tomography
n/a: not provided
Rad: Radiography

Table 8. Mean ± standard deviation of aLDFA, mLDFA, and FVA in dogs with different grades of MPL.

Dog Breeds [Author]	**Angle**	**MPL 1 (°)**	**MPL 2 (°)**	**MPL 3 (°)**	**MPL 4 (°)**
Pomeranian [Soparat et al., 2012] ^{Rad}	**aLPFA**	98.88 ± 3.87		103.24 ± 5.92	n/a
	mLPFA	101.65 ± 3.14		104.48 ± 4.36	n/a
	FVA	9.38 ± 3.73		13.15 ± 5.50	n/a
Small Breeds [Olimpo et al., 2016] ^{Rad}	**aLPFA**	100 ± 4	95.6 ± 6	98.6 ± 7	107 ± 14.6
	mLPFA	103.3 ± 3	99.8 ± 4.5	103.5 ± 6.2	105 ± 5.6
	FVA	n/a	n/a	n/a	n/a
Toy Poodles [Yasukawa et al., 2016] $^{Rad\ \&\ CT}$	**aLPFA**	n/a	94.3 ± 4.8 ^{Rad} 89.5 ± 3.8 ^{CT}	n/a	110.5 ± 8.5 ^{Rad} 108.1 ± 8.0 ^{CT}
	mLPFA	n/a	99.3 ± 3.9 ^{Rad} 95.0 ± 3.6 ^{CT}	n/a	113.3 ± 5.3 ^{Rad} 111.1 ± 6.9 ^{CT}
	FVA	n/a	4.3 ± 4.8 ^{Rad} 0.6 ± 3.8 ^{CT}	n/a	20.5 ± 8.5 ^{Rad} 18.1 ± 8.0 ^{CT}
English Bulldogs [Lusetti et al., 2017] ^{CT}	**aLPFA**	n/a	100.02 ± 8.41		n/a
	mLPFA	n/a	103.22 ± 4.37		n/a
	FVA	n/a	n/a		n/a
English Staffordshire Bull Terriers [Newman and Voss 2017] ^{CT*}	**aLPFA**	98.62 ± 3.23			
	mLPFA	n/a			
	FVA	n/a			
Small breeds [Garnoeva et al., 2018] ^{Rad} **	**aLPFA**	102 [92–118]	106 [86–129]	109 [84–125	n/a
	mLPFA	102 [96–114]	105 [85–127]	109 [92–119]	n/a
	FVA	13 [7–17]	17 [2–36]	18 [3–27]	n/a
Chihuahuas [Phetkaew et al., 2018] $^{Rad\ \&\ CT}$	**aLPFA**	99.8±4.8 $^{Rad\ CrCd}$ 99.4±5.0 $^{Rad\ CdCr}$ 97.0±4.2 ^{CT}	100.7±3.0 $^{Rad\ CrCd}$ 100.8±3.5 $^{Rad\ CdCr}$ 97.6±3.6 ^{CT}	102.7±3.1 $^{Rad\ CrCd}$ 102.1±5.1 $^{Rad\ CdCr}$ 98.7±4.2 ^{CT}	114.6±11.5 $^{Rad\ CrCd}$ 112.1±13.3 $^{Rad\ CdCr}$ 109.2±9.7 ^{CT}
	mLPFA	101.0±6.3 $^{Rad\ CrCd}$ 102.7±3.3 $^{Rad\ CdCr}$ 100.0±2.0 ^{CT}	103.2±2.0 $^{Rad\ CrCd}$ 103.4±2.5 $^{Rad\ CdCr}$ 101.3±2.5 ^{CT}	104.6±2.2 $^{Rad\ CrCd}$ 104.6±3.0 $^{Rad\ CdCr}$ 102.7±3.3 ^{CT}	113.5±8.0 $^{Rad\ CrCd}$ 112.1±8.8 $^{Rad\ CdCr}$ 111.9±9.3 ^{CT}
	FVA	n/a	n/a	n/a	n/a
Yorkshire Terriers [Žilinčík et al., 2018] ^{Rad}	**aLPFA**	96.13 ± 2.05	97.17 ± 3.44	100.53 ± 2.05	110.23 ± 6.64
	mLPFA	n/a	n/a	n/a	n/a
	FVA	6.13 ± 2.05	6.94 ± 2.70	10.53 ± 2.05	20.26 ± 6.63

* Mean and standard deviation for different grades of MPL (grade 1-4 MPL)
**Results are reported as median [minimum-maximum] in these studies
CdCr: Caudocranial projection
CrCd: Craniocaudal projection
CT: Computed Tomography
n/a: not provided
Rad: Radiography

3.7.4 Quadriceps angle

Q angle is the angle between the long axis of the rectus femoris muscle and patellar ligament and represents the force generated by the quadriceps muscle. Q angle reported being increased in dogs with MPL (Kaiser et al. 2001). Mortari et al. 2009 evaluated pre- and postoperative values of the Q angle in dogs with different grades of MPL and reported a significant pre-operative difference between the dogs with grades 1 and 3 MPL and between the dogs with grades 2 and 3 MPL. The postoperative Q angle was decreased (24.13%) in dogs with grade 3 MPL, nevertheless the difference between pre- and postoperative Q angles were not statistically significant. These results showed that the Q angle was increased in dogs with MPL. Łojszczyk-Szczepaniak et al. 2014 reported standard values (mean ± SD: 17° ± 7.38) in healthy German Shepherd dogs, which was larger than those reported by Kaiser et al. 2001 (mean: 10.7° ± 4.9). In another study, Pinna, and Romagnoli 2017 reported a reference value for Q angle in healthy dogs using radiographs. The population of the dogs was divided into the small breeds (below 15 kg body weight) and medium-large breeds (more than 15kg body weight). Statistically higher Q angle was recorded for small breed dogs in comparison with large breeds. The values reported for small breed dogs were larger than those reported by Kaiser et al. 2001. Garnoeva et al. 2018 reported that the Q angle values in dogs with different grades of MPL were significantly higher than Q angle values in non-affected dogs. The values of the Q angles reported in the literature are shown in table 9.

Table 9. Mean ± standard deviation of the Q angle in healthy dogs and dogs with medial patellar luxation.

Dog Breeds [Author]	**Healthy dogs**	**MPL 1 (°)**	**MPL 2 (°)**	**MPL 3 (°)**	**MPL 4 (°)**
Combination of different breeds	n/a	14.9 ± 7	22.1 ± 6.4	34.4 ± 13.7	34.0 ± 9.4
[Mortari et al., 2009] Rad	18.3 (6.1 – 29.7) ***	n/a	n/a	n/a	n/a
[Pinna & Romagnoli., 2017] Rad*	8.7 (2.7 – 14.8) ***	n/a	n/a	n/a	n/a
[Pinna & Romagnoli., 2017] Rad **					
German Shepherds [Łojszczyk-Szczepaniak et al., 2014] Rad	17° ± 7.38	n/a	n/a	n/a	n/a
Small Breeds [Garnoeva et al., 2018] Rad ***	14 (8-28)	20.5 (14-30)	22 (15-39)	31 (18-46)	n/a

* Dogs with bodyweight below 15 kilograms
** Dogs with bodyweight more than 15 kilogram
*** Results are reported as median [minimum-maximum] in these studies
n/a: not provided
Rad: Radiography

3.7.5 Mechanical axis-femoral angle, stifle mechanical axis deviation and patellar alignments

Dismukes et al. 2008a reported a standardized method for full-limb radiographic determination of the pelvic limb alignments in the frontal plane in dogs with CrCl rupture including a mechanical axis-femoral angle and stifle mechanical axis deviation. No significant difference was reported between the right and left pelvic limbs, between male and female dogs and between tarsal varus and tarsal valgus. The mean and standard deviation for

MAFA (mechanical axis—femur angle) and SMAD (%) (Stifle mechanical axis deviation) in this study were 5.6 ± 1.7 and 3.6 ± 1.1 respectively.

Mostafa et al. 2008 evaluated the reproducibility of radiographic measurements characterizing the proximodistal alignment of the patella in dogs with and without patellar luxation and evaluated the potential contribution of patellar position (alta or baja) to the side of patellar luxation (medial or lateral). The authors concluded that MPL is associated with a relatively long patellar ligament and patella alta in medium to giant breed dogs. LPL is associated with a relatively long proximal tibia and patella baja.

3.8 Femoral alignments in the sagittal plane

3.8.1 Anatomic caudal proximal femoral angle, mechanical caudal proximal femoral angle, Anatomic caudal distal femoral angle, mechanical caudal distal femoral angle and procurvatum angle

Proximal and distal femoral angles in the sagittal plane were evaluated in the few articles. Only three studies were assessed the femoral alignments in the sagittal plane. Yasukawa et al. 2016 evaluated all of these alignments in healthy Toy Poodles and Toy Poodles with grades 2 and 4 MPL using radiography and CT scan. The authors reported no significant difference between healthy and affected dogs for the mentioned values. Phetkaew et al. 2018 evaluated aCdPFA, aCdDFA, PA and reported a significant difference between CT imaging and both craniocaudal and caudocranial radiographs in healthy stifles for measured values. Based on CT scans, the aCdPFA was related to the severity of MPL in Chihuahuas. The results showed that the aCdPFA was significantly decreased in grades 2, 3 and 4 MPL. The results reported by Kara et al. 2018 showed an inverse correlation between AA and aCdDFA; however, no significant difference between male and female dogs was reported for the aCdDFA. The results of measurements of the femoral alignments in the sagittal plane are shown in table 10.

Table 10. Mean ± standard deviation of the aCdPFA, mCdPFA, aCdDFA, mCdDFA and PA reported in the literature.

Dog Breeds [Author]	Angles	Healthy dogs (°)	MPL 1 (°)	MPL 2 (°)	MPL 3 (°)	MPL 4 (°)
Toy Poodles [Yasukawa et al., 2016]	**aCdPFA**	157.3±7.7 Rad 153.3±5.1 CT	n/a	153.3 ± 8.0 Rad 151.6 ± 6.0 CT	n/a	152.5±11.3 Rad 151.7 ±5.6 CT
	mCdPFA	7.5 ± 5.9 Rad 9.6 ± 5.5 CT	n/a	10.6 ± 7.5 Rad 11.3 ± 5.9 CT	n/a	13.4 ± 8.8 Rad 10.4 ± 6.2 CT
	aCdDFA	104.3±2.1 Rad 102.9±3.2 CT	n/a	104.5 ± 5.6 Rad 102.6 ± 3.5 CT	n/a	105.6 ± 6.9 Rad 104.7 ± 5.7 CT
	mCdDFA	107.8±1.9 Rad 108.4±1.7 CT	n/a	107.0 ± 3.7 Rad 107.5 ± 2.6 CT	n/a	107.5 ±1.8 Rad 107.0 ±2.7 CT
	PA	12.7 ± 4.1 Rad 11.2 ± 5.2 CT	n/a	12.7 ± 7.1 Rad 11.1 ± 5.4 CT	n/a	14.2 ± 7.3 Rad 15.8 ± 6.9 CT
Chihuahuas [Phetkaew et al., 2018]	**aCdPFA**	148.5±4.8 Rad 156.4±5.3 CT	152.9±8.4 Rad 155.1±7.8 CT	148.0 ±7.0 Rad 149.6 ± 4.6 CT	152.6±7.0 Rad 148.6±6.8 CT	142.6±8.3 Rad 147.3±6.6 CT
	aCdDFA	103.8±2.6 Rad 106.2±2.4 CT	101.3±1.9 Rad 103.6±2.9 CT	100.0±4.5 Rad 101.8±4.0 CT	100.8±3.3 Rad 102.7±4.4 CT	102.3±5.5 Rad 102.6±6.4 CT
	PA	9.1 ±2.9 Rad 11.7 ±3.4 CT	7.3 ±2.7 Rad 10.1 ±3.4 CT	7.0 ±3.4 Rad 7.5 ±2.9 CT	7.2 ±5.2 Rad 8.4 ±6.2 CT	6.9 ±5.0 Rad 9.9 ±5.6 CT
Different breeds [Kara et al., 2018]	**aCdDFA**	90.51±6.19 CT	n/a	n/a	n/a	n/a

CT: Computed Tomography
n/a: not provided
Rad: Radiography

3.9 Femoral alignments in the transverse plane

3.9.1 Femoral angle of anteversion and femoral neck angle anteversion angle

The femoral angle of anteversion (AA) helps veterinarians to investigate anteversion or retroversion of the femur in the transverse plane. In 1973 Nunamaker et al. reported a method for measurement of AA on axial view radiographs. Radiography is the easiest method to measure the femoral torsion; however, the radiographs are vulnerable to the positioning errors that may affect the measured values. Given that the CT and magnetic resonance imaging (MRI) are reported as gold standards in human medicine, Dudley et al. 2006 described a CT technique for the determination of AA in sound dogs and compared this technique with previously used standard radiography and anatomic preparation. The results showed no significant difference between the three methods. Barnes et al. 2015 reported a good intra- and inter-observer agreement for measurement of AA with CT imaging. In 2016, Savio et al. developed a new method for measurement of AA using 3D polygonal mesh models of canine femora and reported the reference values. Kara et al. 2018 reported a weak inverse correlation between AA and aCdDFA; however, a weak positive correlation between the AA and aLDFA was recorded in this study. In 2018, Longo et al. investigated AA in cadavers of sound dogs using 3D automated computer-aided reconstruction and reported the highest repeatability and reproducibility for this method in comparison with radiography and manual CT reconstructions.

In the study performed by Olimpo et al. 2016 no significant difference reported for AA in small breed dogs with and without MPL using radiographs. The same results were reported by Lusetti et al. 2017, which reported no significant difference for AA in English Bulldogs with and without MPL using CT scans and by Phetkaew et al. 2018, which reported no significant difference for AA in Chihuahuas with and without MPL using CT scans. Contrarily to these studies, Yasukawa et al. 2016 reported significantly lower AA with CT imaging for Toy poodles with grade 4 MPL compared to the grade 2 MPL and healthy Toy poodles. In 2017, Newman and Voss evaluated AA (overall), proximal AA (PAA) and distal AA (DAA) in English Staffordshire Bull Terriers with and without congenital MPL by CT scans and reported significantly decreased AA and DAA in dogs with grades 2 and 3 MPL, which was aligned with the results of the Yasukawa et al. 2016 However, the radiographic study performed by Žilinčík et al. 2018 on Yorkshire Terriers with and without MPL showed that the dogs with grade 4 MPL had significantly lower AA in compare with other groups.

The femoral neck anteversion angle (FNA angle) is used to evaluate the proximal femoral torsion or ante- or retroversion of the femoral neck relative to the diaphysis (Mostafa et al. 2014, Mostafa et al. 2018). FNA angle is an important value to evaluate the transfer of the biomechanical forces from the femur to the acetabulum, therefore it is significant in hip dysplasia. In 1985 Montavon et al. reported a standard biplanar method for measurements of femoral neck anteversion with frontal and sagittal radiographs (FNA angle = Tan α), which was based on geometric and trigonometric relationship between the distance of the center of the head of the femur and anatomic axes of the femur in the frontal plane (y) to the center of the head of the femur and anatomic axes in the sagittal plane (x),($\alpha = \frac{x}{y}$). In 2007, Ginja et al. described a new method for measurement of the FNA angle in Estrela Mountain dogs with CT and compared the results with the standard radiographic biplanar method which was reported by Montavon et al. 1985. The authors reported high inter- and intra-observer ICCs for CT imaging but no significant difference between radiographic biplanar method and CT imaging was recorded. Ragetly et al. 2011 assessed conformation variables of the pelvic limbs of the predisposed and non-predisposed Labrador Retrievers for CrCL diseases with radiographs, CT images and dual-energy X-ray absorptiometry (DEXA) and determined that a combination of TPA and FNA angle that measured on radiographs was optimal for distinguishing predisposed and non-predisposed limbs for CrCL disease in Labrador Retrievers, the authors concluded that the increased TPA and FNA angle may change the stifle joints biomechanics leading to the CrCL rupture. Mostafa et al. 2014 developed a new technique for measurement of the FNA angle on single lateral radiographs and compared this method with biplanar radiography and AA from CT techniques in Labrador Retrievers with and without CrCL rupture. The authors reported that the determination of femoral torsion with a single lateral radiograph can be measured but the results will be inaccurate as only CT identified and localized the site of femoral torsion. A significantly higher AA was recorded for the dogs with CrCl disease using CT imaging, whereas no significant difference between healthy and affected dogs with radiographic methods was reported. Mostafa et al. 2018 evaluated the influence of traditional Reynolds technique has been used to assess femoral anteversion angle (t-FAA) and angled beam projection (a-FAA) methods on the measurements of femoral anteversion angle, furthermore, the authors assessed the correlation between the methods and investigated the influence of these techniques on CrCL disease scores. They reported that both radiographic methods correlated strongly with each other; however, fair and good to excellent intra- and interobserver variabilities were recorded for the t-FAA and a-FFA respectively. The results reported for the AA and FNA angle are shown in table 11.

Table 11. Mean ± standard deviation of the AA and FNA angle reported in the literature.

<table>
<tr><th>Author</th><th>AA (°)</th><th>FNA angle (°)</th></tr>
<tr><td>Montavon et al. 1985</td><td>n/a</td><td>Radiography: 31.3 ± 6.2
Anatomic specimen: 31.6 ± 6.4</td></tr>
<tr><td>Dudley et al. 2006</td><td>Radiography: 16 ± 6.4
CT: 19.6 ± 7.9
Anatomic specimen: 18.9 ± 5.4</td><td>n/a</td></tr>
<tr><td>Ginja et al. 2007</td><td>n/a</td><td>Radiography: 29.9 ± 4.8
CT: 30.4 ± 4.2</td></tr>
<tr><td>Ragetly et al. 2011</td><td>n/a</td><td>Predisposed for CrCL: 33.5 ± 3.5
Non-predispose for CrCL: 26.0 ±5.0</td></tr>
<tr><td>Mostafa et al. 2014</td><td>Healthy (CT): 28.0 ± 4.9
CrCL (CT): 32.8 ± 6.0</td><td><table><tr><th></th><th>Healthy</th><th>CrCL</th></tr><tr><td>Lateral plane radiograph:</td><td>24.7 ± 6.5</td><td>24.7 ± 6.5</td></tr><tr><td>Biplanar plane radiograph:</td><td>26.1 ± 6.4</td><td>30.5 ± 8.6</td></tr><tr><td>Biplanar [1]MC plane radiograph:</td><td>25.5 ± 8.1</td><td>27.8 ± 8.9</td></tr></table></td></tr>
<tr><td>Barnes et al. 2015</td><td>CT: 26.6 ± 7.9</td><td>n/a</td></tr>
<tr><td>Savio et al. 2016</td><td>[2]Radio: 30.2 ± 5.7
[3]Projected planes: 19.1 ± 5.7
3D model: 45.0 ± 4.5</td><td>n/a</td></tr>
<tr><td>Olimpo et al. 2016</td><td>Healthy: 20.4 ± 4.8
MPL 1: 17.8 ± 3.8
MPL 2: 104.6 ± 7.4 *
MPL 3: 15.2 ± 8
MPL 4: 17 ± 0</td><td>n/a</td></tr>
<tr><td>Yasukawa et al. 2016</td><td>Normal (CT): 19.8 ± 4.6
MPL 2 (CT): 16.6 ± 4.8
MPL 4 (CT): 9.6 ± 5.2</td><td>n/a</td></tr>
<tr><td>Lusetti et al. 2017</td><td>Healthy: 11.36 ± 6.41
[4]MPL: 6.90 ± 12.78</td><td>n/a</td></tr>
<tr><td>Newman and Voss 2017</td><td>Healthy: 26.03 ± 3.35
MPL 2-3: 21.94 ± 3.67</td><td>n/a</td></tr>
<tr><td>Kara et al. 2018</td><td>26.86 ± 11.46</td><td>n/a</td></tr>
<tr><td>Longo et al. 2018</td><td>Radio: 23.91 ± 8.3
CT: 24.14 ± 7.6
[5]CAD: 20.44 ± 7.05</td><td>n/a</td></tr>
<tr><td>Mostafa et al. 2018</td><td>n/a</td><td><table><tr><th></th><th>Traditional</th><th>Angled beam</th></tr><tr><td>Healthy</td><td>34.7 ± 4.9</td><td>33.7 ± 4.7</td></tr><tr><td>CrCL disease</td><td>34.3 ± 6.3</td><td>34.1 ±6.7</td></tr></table></td></tr>
<tr><td>Phetkaew et al. 2018</td><td>Healthy: 29.2 ± 6.3
MPL 1: 25.9 ± 7.8
MPL 2: 27.6 ± 6.5
MPL 3: 25.8 ± 6.0
MPL 4: 21.1 ± 5.6</td><td>n/a</td></tr>
<tr><td>Žilinčík et al. 2018</td><td>Healthy: 19.62 ± 2.86
MPL 1: 19.23 ± 1.91
MPL 2: 19.11 ± 2.61
MPL 3: 17.04 ± 2.18
MPL4: 9.23 ± 2.82</td><td>n/a</td></tr>
</table>

* The results reported for MPL grade 2 in this study is not matching with other grades and seems to be a misspelling in the original article

[1]Biplanar magnification corrected anteversion angle plane

[2]Radio: Radiography

[3]Projected plane with the femur inclined at an angle of 25° with a caudal-cranial orientation

[4]Mean and standard deviation for different grades of MPL (grade 1 -4 MPL)

[5]Three-dimensional automated computer-aided design

n/a: not provided

3.10 Tibial alignments frontal plane

In 2007, Dismukes et al. described a standardized method for radiographic measurement of mMPTA and mMDTA in Labrador Retrievers and non-Labradors with CrCL rupture. No significant difference was recorded between the two groups. One year later Dismukes et al. 2008a reported a standardized method for full-limb radiographic determination of the tibial alignments in the frontal plane and reported the values of mMPTA (92.2 ± 1.8), mMDTA (95.9 ± 2.2), mTFA (9.1 ± 2.8), mMTTA ($- 0.58 \pm 2.1$), MAMTA (2.9 ± 1.5), and TMAD (1.21 ± 0.63) in dogs with CrCL rupture. No difference between male and female dogs was reported for any of the mentioned angles. Lambert and Wendelburg 2010 compared tangential caudocranial radiographic projection (tCdCr) and straight caudocranial projection (sCdCr) before and after inducing a varus deformity in the proximal aspect of the tibia. The results showed that mMPTA in tCdCr was statistically different from mMPTA in sCdCr projection for the varus tibiae. The authors concluded that the varus deformity in mMPTA was identified on tCdCr projections whereas it was not identified on sCdCr projections. Fuller et al. 2014 compared the mMPTA, mMDTA, and FPA in dogs with bilateral CrCL rupture and unilateral CrCL rupture with and without subsequent contralateral CrCL rupture as risk factors for subsequent contralateral CrCL rupture. The mentioned angles were not statistically different between the groups. Barnes et al. 2015 evaluated the intra- and inter-observer variability of measurements of the mMPTA in dogs with and without MPL using CT and reported a good intra- and inter-observer agreement. Most of the variance in the measurement of each parameter was attributable to the dog in this study.

Olimpo et al. 2016 investigated mMPTA and mMDTA in small breed dogs with and without MPL by radiographs and reported a significant difference between sound and affected dogs in relation to the mMPTA. The mMPTA in dogs with grade 4 MPL was significantly greater than those in other groups in this study. In the same year, Yasukawa et al. 2016 evaluated mMPTA and mMDTA in Toy Poodles with and without MPL using radiography and CT and reported no significant difference between sound and affected dogs for both methods, which was in contrary with Olimpo et al.'s findings. The study performed by Lusetti et al. 2017, confirmed the results reported for Toy Poodles and concluded no significant difference for mMPTA and mMDTA between healthy English Bulldogs and English Bulldogs with MPL using CT imaging. Newman and Voss 2017 evaluated tibial valgus in English Staffordshire Bull Terriers with and without congenital MPL using CT imaging. The TV angle was defined as the angle between proximal and distal joint orientation lines in the frontal plane.

English Staffordshire Bull Terriers with MPL had significantly decreased TV angle (8.87 ± 2.43) compared to the healthy dogs (11.80 ± 3.11).

In 2018, Garnoeva et al. reported that the dogs with MPL have higher mMPTA and mLPTA compared to the healthy dogs; furthermore, higher mMDTA was reported for the dogs with grade 1 MPL compared to the healthy dogs. No significant difference reported for mLDTA in this study. These results were relevant to the results reported by Olimpo et al. 2016. Phetkaew et al. 2018 evaluated the hind limb alignments in Chihuahuas with and without MPL and compared the results of the radiographic CT methods. The authors reported that the mMPTA and mMDTA with radiography differed significantly with those in CT imaging. The values reported for the mMPTA and mMDTA are shown in table 12.

Table 12. Mean ± standard deviation of the mMPTA and mMDTA reported in the literature.

Author	mMPTA (°)					mMDTA (°)				
Dismukes et al. 2007	93.30 ± 1.78					95.99 ± 2.70				
Dismukes et al. 2008a	92.2 ± 1.8					95.9 ± 2.2				
Lambert &Wendelburg 2010	[1]sCdCr: 93.7 [2]tCdCr: 91.6					n/a				
Fuller et al. 2014	bilateral CrCL	[3]unilateral CrCL	[4]unilateral without			bilateral CrCL	unilateral CrCL	unilateral without		
	93.3 ± 1.8	92.6 ± 2.2	93.1 ± 2.6			95.8 ± 1.9	95.6 ± 1.9	94.9 ± 2.0		
Olimpo et al. 2016	Sound	MPL1	MPL2	MPL3	MPL4	Sound	MPL1	MPL2	MPL3	MPL4
	95.1 ± 3.2	95.1 ± 2.5	94.8 ± 2	97.1 ± 4.7	110.8 ± 12.5	98.1 ± 4.4	96 ± 3.3	97.2 ± 3.9	97.1 ± 3.8	96.2 ± 2.7
Yasukawa et al. 2016		Sound	MPL2	MPL4			Sound	MPL2	MPL4	
	Radio	94.4 ± 3.8	96.9 ± 3.5	[5]NE		Radio	96.5 ± 2.3	94.2 ± 4.4	NE	
	CT	94.8 ± 2.1	94.7 ± 1.7	94.5 ± 4.4		CT	96.5 ± 4.1	95.2 ± 2.4	98.5 ± 4.1	
Lusetti et al. 2017	Healthy: 91.98 ± 4.28 MPL: 93.25 ± 4.34					Healthy: 91.34 ± 2.98 MPL: 92.98 ± 3.01				
[6]Garnoeva et al. 2018	Healthy	MPL1	MPL2	MPL3		Healthy	MPL1	MPL2	MPL3	
	90 [78-108]	90 [81-103]	92 [85-107]	97 [87-110]		90 [75-99]	96 [83-106]	90 [75-103]	90 [79-100]	
Phetkaew et al. 2018		Radio		CT			Radio		CT	
		[7]CrCd	[8]CdCr				CrCd	CdCr		
	Healthy	94 ± 1.0	99.1 ± 2.2	96.3 ± 4.1		Healthy	97.2 ± 3.7	93.4 ± 1.1	94.3 ± 7.8	
	MPL1	96.6 ± 3.1	96.9 ± 3.1	95.8 ± 3.0		MPL1	92.3 ± 4.3	94.8 ± 3.5	92.0 ± 4.7	
	MPL2	94.7 ± 3.3	97.1 ± 3.3	96.7 ± 3.3		MPL2	93.6 ± 3.9	93.3 ± 2.4	92.6 ± 4.4	
	MPL3	96.2 ± 2.3	98.4 ± 2.7	96.7 ± 3.3		MPL3	92.1 ± 2.7	95.0 ± 2.4	91.9 ±2.6	
	MPL4	99.6 ± 7.1	103.1 ± 7.2	102.2 ± 8.5		MPL4	100.3 ± 6.2	97.3 ± 4.2	94.4 ± 3.9	

[1] Straight caudocranial projection
[2] Tangential caudocranial projection
[3]Unilateral CrCL with subsequent contralateral rupture
[4]Unilateral CrCL without subsequent contralateral rupture
[5] Not evaluated
[6] The values are reported as median [range]
[7]Craniocaudal
[8]Caudocranial
n/a: not provided

3.11 Tibial alignments in the sagittal plane

Osmond et al. 2006 investigated the morphology of the proximal portion of the tibia in dogs with and without CrCL rupture. The TPS (Healthy: 23.6 ± 3.4, affected: 31.8 ± 4.1), TPO (Healthy: 25.1 ± 3.6, affected: 34.5 ± 4.7), DPA (Healthy: 4.1 ± 2.2, affected: 6.0 ± 3.3) were evaluated on radiographs in this study. These values differed significantly between dogs with ruptured CrCL and healthy dogs. The TPS and TPO were highly correlated whereas no relationship between TPS and DPA was recorded. In 2008 Dismukes et al. 2008b described a method for determining mCdPTA and mCrDTA in the sagittal plane and reported no difference for measured angles between Labrador Retrievers and non-Labrador Retrievers with CrCL disease. Lambert and Wendelburg 2010 reported no difference for the TPA with tangential caudocranial radiographic projection (tCdCr) and straight caudocranial projection (sCdCr) in sound dogs. Glassman et al. 2011 investigated inter- and intra-observer variability in radiographic measurement of TPA and DPA angle in dogs with CrCL rupture. High inter- and intra-observer agreement reported for TPA and DPA in this study. Ragetly et al. 2011 reported that a combination of measured TPA and FAA (FNA angle) on radiographs was optimal for distinguishing predisposed and non-predisposed limbs for CCL disease in Labrador Retrievers. Vedrine et al. 2013 investigated tibial conformation in healthy Labrador Retrievers and Yorkshire Terriers and compared measured alignments between two breeds. TPA, PTA, Z angle, DPA and rTTW were measured and reference values reported. The authors reported a significant effect of breed on measured values. Labrador Retrievers had a lower TPA, Z angle, DPA and rTTW than Yorkshire Terriers, whereas higher PTA was recorded for Labrador Retrievers compared to the Yorkshire Terriers. The DPA was correlated with TPA, Z angle, and rTTW; in addition, the TPA was also correlated with the Z angle in this study. Fuller et al. 2014 evaluated the TPA, mCdPTA, mCrDTA, and SPA and in dogs with bilateral CrCL rupture, unilateral CrCL rupture with subsequent rupture and unilateral CrCL rupture without subsequent contralateral CrCL rupture. They reported no statically difference between the groups, therefore the mentioned angles were not a risk factor for subsequent contralateral CrCL rupture. Sabanci and Ocal 2014 compared the lateral and medial TPA in sound dogs using radiography and photography. A significant difference between medial TPA and lateral TPA was recorded, further, the difference in the photographic medial TPA between male and female dogs was significant. In the photographic method, a significant difference between medial and lateral TPA was recorded for the male dogs, however, a significant difference was recorded for photographic lateral TPA between dog breeds in this study. In 2015, Aertsens et al. investigated the TPA, Z angle, and rTTW in small and large breed dogs with CrCL disease. The results showed that the small breed dogs have a greater TPA and Z angle than large breed dogs. Sex and neutered status influenced the TPA and Z angle values, whereas no significant effect was observed on the rTTW values. A strong correlation was found between the TPA and the Z angle. Variances were not significantly different between observers, and overall the inter-observer variability was low, suggesting a good inter-observer agreement for measured values. Su et al. 2015 compared TPA in small and large breed dogs. The measurements were performed on radiographs of the dogs with and without CrCL disease. The results showed that small breed dogs have mean TPA 3.1° ± 0.6° higher than large breed dogs, furthermore higher TPAs were recorded for spayed females and castrated males compared to the intact males. Healthy dogs had lower TPAs compared to the dogs with unilateral or bilateral CrCL disease. Witte 2015 assessed proximal tibial alignments including TPA, DPA, PTA, Z angle and rTTW in healthy small breed dogs to investigate optimal extracapsular stabilizing suture attachment sites and stifle joint angle at the time of suture placement and investigated the influence of proximal tibial anatomy on these attachment site anisometry. The author reported an individual variation in the optimal attachment site combination and stifle angle for suture placement, which may influence the consistency of outcomes. Olimpo et al. 2016 reported that the TPA in small breed dogs with grade 4 MPL was significantly greater than those in other groups; however, the mCdPTA in healthy dogs was significantly lower than the dogs with different grades of MPL. No significant difference reported for mCrDTA between the groups. Yasukawa et al. 2016 investigated mCrPTA, mCrDTA, TPA, Z angle and rTTW in Toy Poodles with and without MPL using radiography and CT and reported no significant difference among the healthy and affected dogs on CT and radiographs. In 2017, Guénégo et al. compared repeatability and reproducibility of measurements of tibial AMA angle, TPA, rTTW, and Z angle from radiographs of the predisposed dogs and dogs at low risk of CrCL rupture. Good intra- and inter-observer agreement reported for all measurements in this study; furthermore, a significant difference between the control group and the CrCl rupture group was recorded. In the CrCL rupture group, rTTW was significantly lower than those in the control group but AMA-angle, TPA and Z angle were significantly increased in the CrCL group compared to the control group. Janovec et al. 2017 investigated TPA, PTTA, rTTW, relative body weight and tibial plateau length in small breed dogs with and without CrCL rupture using radiographs. Gender, age, and weight were not significantly different between the two groups of dogs; however, dogs with CrCL rupture had significantly a greater sTPA (TPA as described by Slocum and Slocum) and relative body weight than the control group. Lusetti et al. 2017 reported no significant difference for mCdPTA and mCdDTA in English Bulldogs with and without MPL with CT; whereas, Garnoeva et al. 2018 reported greater mCrPTA in healthy dogs compared to the dogs with grade 3 MPL, Furthermore significant difference was recorded for mCdDTA of the healthy dogs and dogs with grade 2 MPL in this study. Phetkaew et al. 2018 reported a significant difference between radiographs and CT for the mCrDTA in Chihuahuas with grade 2 MPL. Evaluated tibial alignments in the sagittal plane are summarized in table 13.

Table 13. Mean ± standard deviation of the tibial alignments in the sagittal plane.

Dog breed	Study	TPA (°)	DPA (°)	mCdPTA (°)	mCrDTA (°)	Z angle (°)	rTTW (°)
Large breeds	[Osmond et al., 2006] Rad	n/a	Healthy: 4.1 ± 2.2 *CrCl: 6.0 ± 3.3	n/a	n/a	n/a	n/a
	[Dismukes et al., 2008] Rad	n/a	n/a	CrCl: 63 ± 3.9	CrCl: 81.5 ± 4.1	n/a	n/a
	[Lambert & Wendelburg 2010] Rad	Healthy: 25.1	n/a	n/a	n/a	n/a	n/a
	[Glassman et al., 2011] Rad **	CrCl: 27.9 [18.8-41.3]	CrCl: 6.5 ± 2.81	n/a	n/a	n/a	n/a
	[Fuller et al., 2014] Rad	¥ Bi-CrCL: 26.4±3.8 ¥¥ Uni-CrCL: 27.0±3.9 ¥¥ Uni-wo: 28± 3.6	n/a	Bi-CrCL: 63.6± 3.8 Uni-CrCL: 63.0± 3.9 Uni-wo: 62.0± 3.6	Bi-CrCL: 80.5±3.2 Uni-CrCL: 79.7±2.8 Uni-wo: 80.8±3.4	n/a	n/a
	[Aertsens et al., 2015] Rad	CrCl: 24.9 ± 3.9	n/a	n/a	n/a	CrCl: 64.0 ± 4.7	CrCl: 0.80 ± 0.12
	[Su et al., 2015] Rad	Healthy: 26.1 ± 0.8	n/a	n/a	n/a	n/a	n/a
	[Guénégo et al., 2017] Rad **	Healthy: 24.0 [10.40-34.00] CrCL: 27.5 [20.0-42.0]	n/a	n/a	n/a	Healthy: 63.0 [54.0-72.5] CrCL: 64.30 [52.0-83.2]	Healthy: 0.84 [0.69-1.26] CrCL: 0.73 [0.55-0.98]
Labrador Retriever	[Dismukes et al., 2008] Rad	n/a	n/a	CrCl: 63.8 ± 3.7	CrCl: 81.7 ± 4.2	n/a	n/a
	[Ragetly et al., 2011] Rad	Healthy: 25.2 ±2.1 Predisposed: 28.4 ±2.0	n/a	n/a	n/a	n/a	n/a
	[Vedrine et al., 2013] Rad	Healthy: 25 ± 3	Healthy: 4.5 ± 2.3	n/a	n/a	n/a	n/a
Yorkshire Terrier	[Vedrine et al., 2013] Rad	Healthy: 30 ± 4	Healthy: 10.8 ± 4.3	n/a	n/a	n/a	n/a
Medium to large breeds	[Sabanci and Ocal, 2014] Rad	Healthy (medial): 24.0 ± 3.19 Healthy (lateral): 25.5 ± 3.84	n/a	n/a	n/a	n/a	n/a
Small breeds	[Aertsens et al., 2015] Rad	CrCl: 30.1 ± 5.3	n/a	n/a	n/a	CrCl: 70.0 ± 5.6	CrCl: 0.82 ± 0.12
	[Su et al., 2015] Rad	Healthy: 29.2 ± 0.8	n/a	n/a	n/a	n/a	n/a
	[Witte 2015] Rad	Healthy: 32 ± 6.2	Healthy: 10.2 ± 7.3	n/a	n/a	n/a	n/a
	[Olimpo et al., 2016] Rad	Healthy: 24.4 ± 3.0 MPL1: 24.6 ± 3.9 MPL2: 23 ± 3.7 MPL3: 23.2 ± 5 MPL4: 16.6 ± 10.4	n/a	Healthy: 65 ± 3.02 MPL1: 74 ± 4.3 MPL2: 72.5 ± 4.3 MPL3: 74 ± 5.5 MPL4: 69.6 ± 5.2	Healthy: 86.3 ± 1.5 MPL1: 84.6 ± 2.7 MPL2: 82.6 ± 1.5 MPL3: 86.8 ± 2.1 MPL4: 87 ± 0	n/a	n/a
	[Janovec et al., 2017] Rad	Healthy: 29.18 ± 7.28 CrCL: 32.0 ± 5.74	n/a	n/a	n/a	n/a	n/a
	[Garnoeva et al., 2018] Rad **	n/a	n/a	Healthy: 63 [54-84] MPL1: 60 [54-84] MPL2: 61 [29-74]	Healthy: 91 [70-101] MPL1: 89 [70-104] MPL2: 84 [68-108]	n/a	n/a

Table 13 continued in the next page.

				MPL3: 64 [51-77]	MPL3: 90 [76-104]		
Toy Poodles	[Yasukawa et al., 2016]	Healthy ^{Rad}: 27.6 ± 4.7 Healthy ^{CT}: 21.3 ± 3.3 MPL2 ^{Rad}: 28.4 ± 5.3 MPL2 ^{CT}: 21.2 ± 3.4 MPL4 ^{CT}: 22.7 ± 4.2	n/a	n/a	Healthy ^{Rad}: 91.0 ± 4.6 Healthy ^{CT}: 98.5±3.8 MPL2 ^{Rad}: 88.8 ± 2.0 MPL2 ^{CT}: 99.2 ±3.1 MPL4 ^{CT}: 98.6 ±6.4	Healthy ^{Rad}: 63.8 ± 5.2 Healthy ^{CT}: 65.7 ± 4.6 MPL2 ^{Rad}: 64.5 ± 3.9 MPL2 ^{CT}: 66.2 ± 3.8 MPL4 ^{CT}: 67.2 ± 5.8	Healthy ^{Rad}: 0.86 ± 0.08 Healthy ^{CT}: 0.74 ± 0.09 MPL2 ^{Rad}: 64.5 ± 3.9 MPL2 ^{CT}: 66.2 ± 3.8 MPL4 ^{CT}: 67.2 ± 5.8
English Bulldogs	[Lusetti et al., 2017] $^{CT+}$	n/a	n/a	Healthy: 63.25 ± 6.15 MPL: 66.04 ± 10.42	n/a	n/a	n/a
Chihuahua	[Phetkaew et al., 2018]	n/a	n/a	Healthy ^{Rad}: 63.1 ±1.15 Healthy ^{CT}: 65.3 ±2.6 MPL1 ^{Rad}: 63.5 ±4.1 MPL1 ^{CT}: 63.9 ±4.6 MPL2 ^{Rad}: 64.1 ±2.3 MPL2 ^{CT}: 62.3 ±3.5 MPL3 ^{Rad}: 63.9 ±4.1 MPL3 ^{CT}: 62.1 ±5.2 MPL4 ^{Rad}: 65.1 ±3.3 MPL4 ^{CT}: 59.9 ±4.8	Healthy ^{Rad}: 91.9 ±2.4 Healthy ^{CT}: 94.9 ±3.1 MPL1 ^{Rad}: 92.2 ±4.0 MPL1 ^{CT}: 91.7 ±5.1 MPL2 ^{Rad}: 88.0 ±2.3 MPL2 ^{CT}: 91.9 ±4.3 MPL3 ^{Rad}: 91.8 ±4.1 MPL3 ^{CT}: 91.4 ±5.4 MPL4 ^{Rad}: 88.3 ±4.4 MPL4 ^{CT}: 96.4 ±3.7	n/a	n/a

* CrCL: Doge with cranial cruciate ligament disease
** Values are expressed as median [min-max] in these studies
+ Mean and standard deviation for different grades of MPL (grade 1 - 4 MPL)
¥ Bilateral CrCL
¥¥ Unilateral CrCL with subsequent contralateral rupture
¥¥¥ Unilateral CrCL without subsequent contralateral rupture
CT: Computed Tomography
n/a: not provided
Rad: Radiograph

3.12 Tibia alignments in the axial plane

Aper et al., 2005 evaluated tibial torsion in healthy dogs using different measurement methods and compared CT with direct anatomic measurements. Tibial torsion angles were calculated from the combination of proximal and distal axis inducing TC-CnT (transcondylar and distal cranial tibial axis pair), TC–CdT (transcondylar and distal caudal tibial axis pair), CdC–CnT (caudal condylar and distal cranial tibial axis pair) and CdC–CdT (caudal condylar and distal caudal tibial axis pair). The results demonstrated no significant difference for the torsion angle between the direct photographic and CT method for any pair of proximal and distal axes. Fitzpatrick et al. 2012 evaluated the influence of tibial torsion, age and sex on MPL in Yorkshire terriers with and without MPL using CT. The tibial torsion angle in this study was defined as the difference between the transcondylar axis (TC) and the distal cranial tibial angle (CnT). The authors concluded that body weight squared, TTA, and age affect MPL grade, suggesting that a tibial torsional may contribute to the development of MPL in dogs. Barnes et al. 2015 reported a good intra- and inter-observer agreement for measurements of the crural torsion angle (CTA) in dogs with and without MPL on CT. In 2016, Hette et al. described a protocol for the measurement of torsion of the medial cortex of the tibia using CT multiplanar reconstructions in chondrodystrophic and non-chondrodystrophic dogs. A significant difference was recorded for the mean medial tibial cortex (MTMC) between chondrodystrophic (23°) and non-chondrodystrophic (26°) dogs. The authors reported that 26° of internal torsional tibial plate pre-contouring may be appropriate for non-chondrodystrophic dogs. Yasukawa et al. 2016 reported higher TTA in Toy Poodles with grade 4 MPL compared to the healthy Toy Poodles, the same result was reported in 2018 by Phetkaew et al. for the Chihuahuas with grade 4 MPL. These results were contrary to the studies performed by Lusetti et al. 2017 and Newman and Voss 2017. Lusetti et al., 2017 reported no significant difference for TTA in English Bulldogs with and without MPL. Newman and Voss 2017 demonstrated no significant difference for TTA in English Staffordshire Bull Terriers with and without MPL. All of the mentioned studies were reported the TTA with CT. The results of the TTA is shown in table 14.

Table 14. Mean ± standard deviation of the tibial torsion angle reported in the literature.

Author	**TTA (°)**			
[1]Aper et al. 2005	[2]TC-CnT: 4.15 ± 4.33 [3]TC-CdT: -12.10 ± 3.99 [4]CdC-CnT: -4.85 ± 5.19 [5]CdC-CdT: -21.10 ± 5.01			
Fitzpatrick et al. 2012	Healthy	MPL1	MPL2	MPL3
	9.1 ± 4.1	9.2 ± 6.2	8.6 ± 5.8	6.7 ± 4.2
Yasukawa et al. 2016	Healthy	MPL 2	MPL 4	
	11.3 ± 4.3	13.0 ± 7.9	32.8 ± 7.9	
Lusetti et al. 2017	Healthy: 4.0 ± 8.8 MPL: 5.92 ± 7.37			
Newman and Voss 2017	Healthy: 6.82 ± 5.6 MPL: 5.47 ± 4.8			

[1] Reported values with CT in healthy dogs, negative or positive values describe the angular orientation of the distal tibial axis with respect to the proximal axis
[2]TC-CnT: transcondylar and distal cranial tibial axis pair
[3]TC–CdT: transcondylar and distal caudal tibial axis pair
[4]CdC–CnT: caudal condylar and distal cranial tibial axis pair
[5]CdC–CdT: caudal condylar and distal caudal tibial axis pair

4 Discussion

This review was carried out on the previously done studies to assess the femoral and tibial conformations in dogs. The main goals of this study were to summarize the results and values reported in the literature and settle standard values for different dog breeds; however, to evaluate the normal alignments, normal variations and pathologic alignments in the dogs.

Investigations on the ICA in most of the articles had the same and homogenous results. According to the articles, no significant difference was recorded for the dogs with and without MPL, as well as dysplastic and non-dysplastic dogs (Sarierler 2004, Soparat et al. 2012, Olimpo et al. 2016, Yasukawa et al. 2016, Lusetti et al. 2017, Newman and Voss 2017, Phetkaew et al. 2018, Žilinčík et al. 2018), whereas one study reported higher ICA for the dogs with grades 2 and 3 MPL (Garnoeva et al. 2018). Studies on healthy dogs showed a significant difference between some of the breeds but not all of them. Most of these differences were identified between large breed dogs (Tomlinson et al. 2007, Sarierler 2004) whereas no study compared ICA between healthy small breed dogs. It is deduced that the ICA does not differ in dogs with and without MPL, thus some differences exist between different breeds.

Except for one study (Žilinčík et al. 2018), the aLPFA and mLPFA between healthy dogs and dogs with MPL had no significant differences (Olimpo et al. 2016, Yasukawa et al. 2016, Lusetti et al. 2017, Garnoeva et al. 2018). Furthermore, no significant difference was recorded between the dogs with CrCL rupture (Dismukes et al. 2008a). Measured aLPFAs and mLPFAs have differed between some of the large breed dogs (Tomlinson et al. 2007), thus further investigations are required to assess the influence of the breeds on measured values. According to these results, it could be presupposed that these alignments may differ between some breeds but MPL does not influence the aLPFA and mLPFA. Contrary to the proximal femoral alignments, aLDFA, mLDFA, and FVA were correlated to the MPL and higher values were recorded in the dogs with higher grades of MPL (Soparat et al. 2012, Olimpo et al. 2016, Yasukawa et al. 2016, Lusetti et al. 2017, Newman and Voss 2017, Garnoeva et al. 2018, Phetkaew et al. 2018, Žilinčík et al. 2018). Only in one study, a significant difference was recorded between some of the large breed dogs (Tomlinson et al. 2007), therefore it needs to be investigated if distal femoral alignments are related to the dog breeds. Measured Q angles in the articles were correlated with the severity of MPL as well (Mortari et al. 2009, Garnoeva et al. 2018, Kaiser et al. 2001). A significant difference was reported between small and large breed dogs for Q angle (Pinna and Romagnoli 2017), but more studies are needed to confirm this finding.

Only a few articles were focused on proximal and distal femoral alignments in the sagittal plane. Two different findings were reported for aCdPFA, mCdPFA, aCdDFA, mCdDFA and PA in dogs with MPL. In one study no significant difference was recorded between healthy and MPL affected dogs (Yasukawa et al. 2016), whereas in another study significantly decreased aCdPFA was reported in dogs with MPL (Phetkaew et al. 2018). According to these findings, an accurate deduction cannot be expected, and further investigation should be done to reach accurate results. A similar condition is valid for AA too. Evaluation of the AA had variable results, some articles reported a significant correlation between AA and grade of MPL (Yasukawa et al. 2016, Newman and Voss 2017, Žilinčík et al. 2018) and measured AAs were decreased in dogs with MPL in these studies, whereas some others rejected any significant difference between AA and grade of MPL (Olimpo et al. 2016, Lusetti et al. 2017, Phetkaew et al. 2018).

As reported before evaluation of the tibial alignments in frontal plane showed a significant difference between the healthy dogs and the dogs with MPL. Higher mMPTA, mMDTA, and TV were recorded for the dogs with MPL in these studies (Olimpo et al. 2016, Newman and Voss 2017, Garnoeva et al. 2018, Phetkaew et al. 2018), only in two articles no difference between sound and affected dogs was recorded (Yasukawa et al. 2016, Lusetti et al. 2017). These findings underlining the relationship between tibial varus or valgus deformity and MPL.

Evaluation of the tibial alignments in the sagittal plane had different outcomes. According to the literature a significant difference was recorded between small and large breed dogs regarding the TPA (Vedrine et al. 2013, Aertsens et al. 2015, Su et al. 2015), furthermore, most of the studies showed a significant difference between the TPA of healthy dogs and dogs with different grades of MPL or CrCL rupture (Su et al. 2015, Olimpo et al. 2016, Guénégo et al. 2017, Janovec et al. 2017), whereas in few studies no significant difference was recorded (Fuller et al. 2014, Yasukawa et al. 2016). Investigated studies on DPA had reported a significant difference between healthy dogs and dogs with CrCL rupture (Osmond et al. 2006), additionally, the DPA has differed between small and large breed dogs (Vedrine et al. 2013). Z angle has significantly differed between small and large breed dogs (Vedrine et al. 2013, Aertsens et al. 2015) and non-affected and affected dogs with CrCl rupture (Guénégo et al. 2017), despite the dogs with CrCl rupture, the Z angle has not differed between sound dogs and dogs with MPL (Yasukawa et al. 2016). The results reported for rTTW were not homogenous in included studies, in some cases, a significant difference was recorded between sound and CrCL ruptured dogs (Guénégo et al. 2017) but it was rejected in another study (Janovec et al. 2017), however, no significant difference was recorded between MPL affected and healthy dogs (Yasukawa et al. 2016). The results of the several studies which investigated mCrPTA, mCrDTA, mCdPTA, and mCdDTA, showed no significant difference between healthy dogs and dogs affected with MPL or CrCL rupture (Dismukes et al. 2008b, Fuller et al. 2014, Yasukawa et al. 2016, Lusetti et al. 2017), contrary to these findings in two studies significant difference was seen (Garnoeva et al. 2018, Phetkaew et al. 2018).

In conclusion, distal femoral alignments in the frontal plane (aLDFA, mLDFA, FVA, and Q angle) and tibial alignments in the frontal plane (mMPTA, mMDTA, and TPA) corresponded to the severity of the MPL. The difference between the affected and non-affected dogs with CrCL rupture was limited to the proximal tibial alignments in the sagittal plane including TPA, Z angle and DPA, which shows the significance of the proximal tibial conformations in dogs with CrCL rupture. Statistically, a significant difference was recorded between some of the dog breeds for different angles but in the same time these results were not valid between other breeds, most of the differences were recorded between large breeds, or between large and small breeds, whereas no comparison was done between small breed dogs. The number of articles that evaluated the influence of the body size, anatomy or breed on the measured alignments is low so that no strong conclusion could be done about this theme. Further investigations should be done to determine the influence of the breed on hind limb conformations, and the occurrence of the related orthopedic disease.

5 Acknowledgment

All radiographic images used in this study were from the University Clinic for Small Animals, Diagnostic Imaging, University of Veterinary Medicine, Vienna. The authors are grateful to Prof. Dr. Sibylle Kneissl and Mr. Johann Ryschawy for preparing the radiographs.

6 Abstract

Evaluation of the limb conformations and clinical goniometry were always important topics in veterinary orthopedics. Using standard measurement methods provide reliable values for the surgeons and allow them to use the reported scales in the literature. The aims of this review were (1) to report standard values in different breeds, (2) to compare the measured values in dogs with and without different orthopedic diseases and (3) to evaluate the accuracy of the reported protocols. The standard guideline reported by Moher et al. 2009 for reporting systematic reviews was used in this study. All articles were collected by screening the databases Scopus, PubMed, and Web of the Science. According to the purpose of the studies, articles were classified into studies which reported standard values and methods (16 articles), studies with a focus on values between sound and diseased dogs (21 articles) and studies with a focus on the accuracy of the methods or tools (14 articles). The number of the measured femoral and tibial alignments in the included articles was 17 and 38 respectively. Statistically, a significant difference was recorded between the standard values of some dog breeds but not all of them. Evaluation of the articles showed that the distal femoral alignments in the frontal plane (aLDFA, mLDFA, FVA, and Q angle) and tibial alignments in the frontal plane (mMPTA, mMDTA) corresponded to the severity of the MPL. The difference between the affected and non-affected dogs with CrCL disease was limited to the TPA, Z angle and DPA. Therefore, we found some differences in the evaluated values between healthy and affected dogs. In most of the articles good or even high intra- and inter-observer agreements were recorded for radiographic and CT measurements. Results of the CT and 3D measurements or combination of them were more accurate than those reported for other methods but statically no significant difference was reported between radiographic and CT methods for most of the measured alignments (FVA, ICA, FNA angle); however, no significant difference was reported between radiographic and cadaveric measurements for some of the alignments (FVA, aLDFA). In conclusion, further investigations should be done to determine the influence of the breed on hind limb conformations, and the occurrence of the related orthopedic disease.

7 Zusammenfassung

Die Beurteilung von Gliedmassenstellungen und die klinisch angewandte Goniometrie sind nicht nur in der Humanorthopädie, sondern auch in der Veterinärorthopädie ein wichtiges Thema. Die Verwendung von Standardmessmethoden liefert dem Chirurgen zuverlässige Werte und ermöglicht so standardisierte Daten als Vergleichswerte aus der Literatur heranzuziehen. Die Ziele dieser Studie sind (1) die Berichterstattung über Standardwerte bei verschiedenen Rassen, (2) der Vergleich der Messwerte bei Hunden mit und ohne orthopädischer Erkrankungen und (3) die Beurteilung der Genauigkeit der berichteten Protokolle. In dieser Studie wurde, die von Moher et al. 2009 veröffentlichte Standardrichtlinie zur Berichterstattung über systematische Übersichtsarbeiten verwendet. Alle für diese Arbeit verwendeten Artikel wurden aus den Datenbanken Scopus, PubMed und Web of the Science gesammelt. Die daraus erhaltenen Artikel wurden je nach Studiendesign in drei Studiengruppen unterteilt. Gruppe 1 sind Studien, die von Standardwerten und -methoden berichteten (16 Artikel), Gruppe 2 sind Studien mit dem Fokus auf den Vergleich von Winkelmessungen zwischen gesunden und kranken Hunden (21 Artikel) und Gruppe 3 sind Studien mit Fokus auf Genauigkeit der Messmethoden und der angewandten bildgebenden Verfahren (14 Artikel). Die Messungen wurden in der Frontal-, der Lateral- und der Transversalebenen durchgeführt. Insgesamt wurden 17 unterschiedliche Winkelmessungen am Femur und 38 unterschiedliche Winkelmessungen an der Tibia für die Beurteilung von Gliedmaßenstellungen (normal, normale Varianten und pathologisch) verwendet.

Bei der Beurteilung von Standardwerten bei verschiedenen Rassen wurde statistisch ein signifikanter Unterschied zwischen einigen der Hunderassen festgestellt, jedoch nicht bei allen untersuchten. Die Auswertung der Artikel mit und ohne orthopädischen Erkrankungen ergab, dass die in der Frontalebene am distalen Femur (aLDFA, mLDFA, FVA und Q-Winkel), wie proximalen und distalen Tibia (mMPTA, mMDTA) gemessenen Winkel mit dem Schweregrad der mediale Patellaluxation korrelieren. Der Unterschied zwischen den betroffenen und nicht betroffenen Hunden mit kranialer Kreuzbandriss beschränkte sich auf den TPA-, Z-Winkel und DPA. Bei den Auswertungen der Messergebnisse innerhalb der Untersucher und zwischen den Untersuchern wurde in den meisten Artikeln eine gute bis sehr gute Übereinstimmung bei den Röntgen- und CT-Untersuchungen festgestellt. Obwohl festgestellt wurde das CT und 3D Messmethoden oder eine Kombination davon anderen Methoden überlegen sind, wurde jedoch für die am häufigsten gemessenen Werte (FVA, ICA, FNA Winkel) keine statistische Signifikanz zwischen Röntgen- und CT-Winkelmessung beschrieben. Bei einigen Winkeln (FVA, aLDFA) konnte auch kein signifikanter Unterschied zwischen Röntgen- und Kadavermessungen berichtet werden. Zusammenfassend ist zu sagen, dass weitere Untersuchungen durchgeführt werden sollten, um den Einfluss der Rassen in Verbindung mit orthopädischen Erkrankungen auf die Messergebnisse der Hintergliedmaßenstellungen einschätzen zu können.

8 References

Aertsens A, Alvarez JR, Poncet CM, Beaufrère H, Ragetly GR. 2015. Comparison of the tibia plateau angle between small and large dogs with cranial cruciate ligament disease. Veterinary and Comparative Orthopaedics and Traumatology. 28(06): 385-90.

Altunatmaz K, Ozsoy S, Guzel O. 2007. Bilateral pes valgus in an Anatolian Sheepdog. Vet Comp Orthop Traumatol. (20): 241–244.

Aper R, Kowaleski MP, Apelt D, Tod Drost W, Dyce J. 2005. Computed tomographic determination of tibial torsion in the dog. Veterinary Radiology & Ultrasound. May 46(3):187-91.

Barnes DM, Anderson AA, Frost C, Barnes J. 2015. Repeatability and reproducibility of measurements of femoral and tibial alignment using computed tomography multiplanar reconstructions. Veterinary surgery. Jan;44(1): 85-93.

Burton NJ, Owen MR. 2007. Limb alignment of pes valgus in a giant breed dog by plate-rod fixation. VetComp Orthop Traumatol. (20): 236–240.

Conzemius MG, Smith GK, Brighton CT, Marion MJ, Gregor TP. 1994. Analysis of physeal growth in dogs, using biplanar radiography. American journal of veterinary research. Jan 55(1):22-7.

Dismukes DI, Fox DB, Tomlinson JL, Cook JL, Essman SC. 2008. Determination of pelvic limb alignment in the large-breed dog: a cadaveric radiographic study in the frontal plane. Veterinary surgery. Oct 37(7):674-82. (a)

Dismukes DI, Tomlinson JL, Fox DB, Cook JL, Song KJ. 2007. Radiographic measurement of the proximal and distal mechanical joint angles in the canine tibia. Veterinary surgery. Oct 36(7):699-704.

Dismukes DI, Tomlinson JL, Fox DB, Cook JL, Witsberger TH. 2008. Radiographic measurement of canine tibial angles in the sagittal plane. Veterinary surgery. Apr 37(3): 300-5. (b)

Dudley RM, Kowaleski MP, Drost WT, Dyce J. 2006. Radiographic and computed tomographic determination of femoral varus and torsion in the dog. Veterinary Radiology & Ultrasound. Oct 47(6): 546-52.

Fitzpatrick CL, Krotscheck U, Thompson MS, Todhunter RJ, Zhang Z. 2012. Evaluation of tibial torsion in Yorkshire Terriers with and without medial patellar luxation. Veterinary Surgery. Nov;41(8): 966-72.

Fuller MC, Kapatkin AS, Bruecker KA, Holsworth IG, Kass PH, Hayashi K. 2014. Comparison of the tibial mechanical joint orientation angles in dogs with cranial cruciate ligament rupture. The Canadian Veterinary Journal. Aug;55(8): 757.

Garnoeva R, Roydev R, Paskalev M, Peichamperi M. 2018. Radiographic measures of pelvic limb malalignment in small breed dogs with various grades of medial patellar luxation. Comparative Clinical Pathology. Nov 1;27(6): 1551-5.

Ginja MM, Gonzalo-Orden JM, Jesus SS, Silvestre AM, Llorens-Pena MP, Ferreira AJ. 2007. Measurement of the femoral neck anteversion angle in the dog using computed tomography. The Veterinary Journal. Sep 1;174(2): 378-83.

Glassman M, Hofmeister E, Weh JM, Roach W, Torres B, Johnston S, Budsberg S. 2011. Radiographic quantitative assessment of caudal proximal tibial angulation in 100 dogs with cranial cruciate ligament rupture. Veterinary Surgery. Oct;40(7): 830-8.

Guénégo L, Payot M, Charru P, Verwaerde P. 2017. Comparison of tibial anatomical-mechanical axis angle between predisposed dogs and dogs at low risk for cranial cruciate ligament rupture. The Veterinary Journal. Jul 1;(225): 35-41.

Hauptman J, Prieur WD, Butler HC, Guffy MM. 1979. The angle of inclination of the canine femoral head and neck. Veterinary Surgery. Jul;8(3): 74-7.

Hette K, Anderson AA, Barnes DM. 2016. Assessing torsion of the medial cortex of the canine tibia using computed tomography multiplanar reconstruction. Journal of Small Animal Practice. May 57(5): 234-9.

Hulse DA. 1993. Medial patellar luxation in the dog. In: Disease Mechanisms in Small Animal Surgery.2nd ed. Bojrab MJ.(ed). Philadelphia: Lea & Febiger, 808-817.

Jackson GM, Wendelburg KL. 2012. Evaluation of the effect of distal femoral elevation on radiographic measurement of the anatomic lateral distal femoral angle. Veterinary Surgery. Nov 1;41(8): 994-1001.

Jaeger GH, Marcellin-Little DJ, Ferretti A. 2007. Morphology and correction of distal tibial valgus deformities. J Small Anim Pract. (48): 678–682.

Janovec J, Kyllar M, Midgley D, Owen M. 2017. Conformation of the proximal tibia and cranial cruciate ligament disease in small breed dogs. Veterinary and Comparative Orthopaedics and Traumatology. 30(03): 178-83.

Johnson SG, Hulse DA, Van Gundy TE, Green RW. 1989. Corrective Osteotomy for Pes Varus in the Dachshund. Vet Surg. (18): 373–379.

Kaiser, S., Cornely, D., Golder, W., Garner, M., Waibl, H., & Brunnberg, L. 2001. Magnetic resonance measurements of the deviation of the angle of force generated by contraction of the quadriceps muscle in dogs with congenital patellar luxation. Veterinary surgery. 30(6): 552-558.

Kara ME, Sevil-Kilimci F, Dilek ÖG, Onar V. 2018. Proximal and distal alignment of normal canine femurs: A morphometric analysis. Annals of Anatomy-Anatomischer Anzeiger. May 1;(217):125-8.

Kettelkamp DB, Hillberry BM, Murrish DE, Heck DA. 1988. Degenerative arthritis of the knee secondary to fracture malunion. Clinical orthopaedics and related research. Sep (234): 159-69.

Lambert RJ, Wendelburg KL. 2010. Determination of the mechanical medial proximal tibial angle using a tangential radiographic technique. Veterinary surgery. Feb 39(2): 181-6.

Lojszczyk-Szczepaniak AN, Silmanowicz P, Balicki I. 2014. Radiological evaluation of the quadriceps angle (Q angle) in German Shepherd Dogs. Med. Weter. 70(1): 46.

Longo F, Nicetto T, Banzato T, Savio G, Drigo M, Meneghello R, Concheri G, Isola M. 2018. Automated computation of femoral angles in dogs from three-dimensional computed tomography reconstructions: Comparison with manual techniques. The Veterinary Journal. Feb 1;(232): 6-12.

Lusetti F, Bonardi A, Eid C, De Bellesini AB, Martini FM. 2017. Pelvic limb alignment measured by computed tomography in purebred English Bulldogs with medial patellar luxation. Veterinary and Comparative Orthopaedics and Traumatology. 30(03): 200-8.

Marretta SM, Schrader SC. 1983. Physeal injuries in the dog: a review of 135 cases. J Am Vet Med Assoc. (182): 708–710.

McCarthy PE. 1998. Bilateral pes valgus deformity in a Shetland Sheepdog. Vet Comp Orthop Traumatol. (11): 197–199.

Miles JE, Mortensen M, Svalastoga EL, Eriksen T. 2015. A comparison of anatomical lateral distal femoral angles obtained with four femoral axis methods in canine femora. Veterinary and Comparative Orthopaedics and Traumatology. May;28(03): 193-8.

Moher D, Liberati A, Tetzlaff J, Altman DG, Prisma Group. 2009. Preferred reporting items for systematic reviews and meta-analyses: the PRISMA statement. PLoS medicine. Jul 21;6(7): e1000097.

Montavon PM, Hohn RB, Olmstead ML, Rudy RL. 1985. Inclination and anteversion angles of the femoral head and neck in the dog evaluation of a standard method of measurement. Veterinary Surgery. Oct;14(4): 277-82.

Morgan PW, Miller CW. 1994. Osteotomy for correction of premature growth plate closure in 24 dogs. Vet Comp Orthop Traumatol. (7):129–135.

Mortari AC, Rahal SC, Vulcano LC, da Silva VC, Volpi RS. 2009. Use of radiographic measurements in the evaluation of dogs with medial patellar luxation. The Canadian Veterinary Journal. Oct;50(10): 1064.

Mostafa AA, Cunningham DP, Boudrieau RJ, Kowaleski MP, Griffon DJ. 2018. Influence of radiographic techniques on the measurement of femoral anteversion angles and a conformation score of pelvic limbs in L abrador retrievers. Veterinary Surgery. Apr;47(3): 421-30.

Mostafa AA, Griffon DJ, Thomas MW, Constable PD. 2008. Proximodistal alignment of the canine patella: radiographic evaluation and association with medial and lateral patellar luxation. Veterinary Surgery. Apr 37(3): 201-11.

Mostafa AA, Griffon DJ, Thomas MW, Constable PD. 2014. Radiographic evaluation of femoral torsion and correlation with computed Tomographic techniques in Labrador retrievers with and without cranial cruciate ligament disease. Veterinary surgery. Jul;43(5): 534-41.

Nelligan MR, Wheeler JL, Lewis DD, Thompson MS. 2007. Bilateral correction of metatarsal rotation in a dog using circular external skeletal fixation. Australian veterinary journal. Aug 85(8):332-6.

Newman M, Voss K. 2017. Computed tomographic evaluation of femoral and tibial conformation in English Staffordshire Bull Terriers with and without congenital medial patellar luxation. Veterinary and Comparative Orthopaedics and Traumatology. 30(03): 191-9.

Nunamaker DM, Biery DN, Newton CD. 1973. Femoral neck anteversion in the dog: its radiographic measurement. Veterinary Radiology. Jan;14(1): 45-8.

Olimpo M, Piras LA, Peirone B. 2016. Pelvic limb alignment in small breed dogs: a comparison between affected and free subjects from medial patellar luxation. Veterinaria Italiana. 52(1):45-50.

Osmond CS, Marcellin-Little DJ, Harrysson OL, Kidd LB. 2006. Morphometric assessment of the proximal portion of the tibia in dogs with and without cranial cruciate ligament rupture. Veterinary Radiology & Ultrasound. Mar 47(2):136-41.

Oxley B, Gemmill TJ, Pink J, Clarke S, Parry A, Baines S, Malcolm McKee W. 2013. Precision of a novel computed tomographic method for quantification of femoral varus in dogs and an assessment of the effect of femoral malpositioning. Veterinary Surgery. Aug;42(6): 751-8.

Paley D. 2003. Principles of deformity correction. Berlin: Springer-Verlag.

Palmer RH, Ikuta CL, Cadmus JM. 2011. Comparison of femoral angulation measurement between radiographs and anatomic specimens across a broad range of varus conformations. Veterinary Surgery. Dec;40(8): 1023-8.

Perry KL, Adams RJ, Andrews SJ, Tewson C, Bruce M. 2017. Impact of femoral varus on complications and outcome associated with corrective surgery for medial patellar luxation. Veterinary and Comparative Orthopaedics and Traumatology. 30(04): 288-98.

Phetkaew T, Kalpravidh M, Penchome R, Wangdee C. 2018. A Comparison of Angular Values of the Pelvic Limb with Normal and Medial Patellar Luxation Stifles in Chihuahua Dogs Using Radiography and Computed Tomography. Veterinary and Comparative Orthopaedics and Traumatology. Feb;31(02): 114-23.

Pinna S, Pizzuti E, Carli F. 2013. Effects of intertrochanteric varus osteotomy on Norberg angle and percent coverage of the femoral head in displastic dogs. Journal of veterinary science. Jun 1;14(2): 185-91.

Pinna S, Romagnoli N. 2017. Radiographic measurement of the quadriceps angle in dogs. PloS one. Oct 12;12(10): e0185833.

Ragetly CA, Evans R, Mostafa AA, Griffon DJ. 2011. Multivariate analysis of morphometric characteristics to evaluate risk factors for cranial cruciate ligament deficiency in Labrador retrievers. Veterinary Surgery. Apr;40(3): 327-33.

Ramadan RO, Vaughan LC. 1979. Disturbance in the growth of the tibia and femur in dogs. Vet Rec. (104):433–435.

Rumph PF, Hathcock JT. 1990. A symmetric axis-based method for measuring the projected femoral angle of inclination in dogs. Veterinary Surgery. Sep;19(5): 328-33.

Sabanci SS, Ocal MK. 2014. Lateral and medial tibial plateau angles in normal dogs. Veterinary and Comparative Orthopaedics and Traumatology. 27(02): 135-40.

Sarierler M. 2004. Comparison of femoral inclination angle measurements in dysplastic and nondysplastic dogs of different breeds. Acta Veterinaria Hungarica. Apr 1;52(2): 245-52.

Savio G, Baroni T, Concheri G, Baroni E, Meneghello R, Longo F, Isola M. 2016. Computation of Femoral Canine Morphometric Parameters in Three-Dimensional Geometrical Models. Veterinary Surgery. Nov 45(8): 987-95.

Soparat C, Wangdee C, Chuthatep S, Kalpravidh M. 2012. Radiographic measurement for femoral varus in Pomeranian dogs with and without medial patellar luxation. Veterinary and Comparative Orthopaedics and Traumatology. 25(03):197-201.

Su L, Townsend KL, Au J, Wittum TE. 2015. Comparison of tibial plateau angles in small and large breed dogs. The Canadian Veterinary Journal. Jun;56(6): 610.

Swiderski JK, Radecki SV, Park RD, Palmer RH. 2008. Comparison of radiographic and anatomic femoral varus angle measurements in normal dogs. Veterinary surgery. Jan;37(1): 43-8.

Tomlinson J, Fox D, Cook JL, Keller GG. 2007. Measurement of femoral angles in four dog breeds. Veterinary Surgery. Aug 36(6): 593-8.

Vaughan LC. 1976. Growth plate defects in dogs. Vet Rec. (98): 185-189.

Vedrine B, Guillemot A, Fontaine D, Ragetly GR, Etchepareborde S. 2013. Comparative anatomy of the proximal tibia in healthy Labrador Retrievers and Yorkshire Terriers. Veterinary and Comparative Orthopaedics and Traumatology. 26(04): 266-70.

Witte PG. 2015. Tibial anatomy in normal small breed dogs including anisometry of various extracapsular stabilizing suture attachment sites. Veterinary and Comparative Orthopaedics and Traumatology. 28(05): 331-8.

Yasukawa S, Edamura K, Tanegashima K, Seki M, Teshima K, Asano K, Nakayama T, Hayashi K. 2016. Evaluation of bone deformities of the femur, tibia, and patella in Toy Poodles with medial patellar luxation using computed tomography. Veterinary and Comparative Orthopaedics and Traumatology. 29(01):29-38.

Žilinčík M, Hluchý M, Takáč L, Ledecký V. 2018. Comparison of Radiographic Measurements of the Femur in Yorkshire Terriers with and without Medial Patellar Luxation. Veterinary and Comparative Orthopaedics and Traumatology. Jan;31(01): 017-22.